METRIC

MIL-STD-1809 (USAF)
15 FEB 91

MILITARY STANDARD

# SPACE ENVIRONMENT FOR USAF SPACE VEHICLES

AMSC N/A

FSC 1810

DISTRIBUTION STATEMENT A: Approved for public release; distribution is unlimited

DEPARTMENT OF THE AIR FORCE
Washington, D.C. 20360

MIL-STD-1809 (USAF)

Space Environment for USAF Space Vehicles

1. This military standard is approved for use within the Department of the Air Force, and is available for use by all Departments and Agencies of the Department of Defense.

2. Beneficial comments (recommendations, additions, deletions) and any pertinent data which may be of use in improving this document should be addressed to:

USAF Space Systems Division, SSD/SDMS
P. o. BOX 92960
Worldway Postal Center
Los Angeles, CA 90009-2960

by using the self-addressed Standardization Document Improvement Proposal (DD Form 1426) appearing at the end of this document or by letter.

# FOREWORD

This Standard addresses the natural unperturbed space environment. It is a compilation of the space environment data obtained from the most authoritative contemporary sources available at the time of compilation. This standard establishes the time-sensitive and orbit-sensitive parameters for the naturally occuring environments. The standard is intended to:

a) Ensure that space environmental interactions are considered and incorporated into the design of space systems and subsystems.

b) Provide a basis for evaluating the hardness of space systems and subsystems against the space environmental interactions.

Space vehicles operating in the space environment experience various effects caused by the vacuum, radiation, and particulate environments, as well as inertial effects. These effects are not specifically addressed in this standard, but should be included in the analyses of the effects of the environment on the space system, to the extent applicable.

This standard does not address effects of human operations in space such as orbiting space debris, transmitter radiations, fluid discharges from space vehicles, outgassing, or surface contamination. Neither does it address the interaction between the environment and an orbiting space vehicle, such as atomic oxygen burning of surface materials, surface glow, plasma waves generated by the presence of the space vehicle, space vehicle charging, or orbital dynamics. Nor, finally, does it address the effects of the environment on the space vehicle and subsystems, such as ionizing radiation damage, single event upsets in electronics, or backgrounds such as luminescence and Cerenkov radiation in optical materials. It does, however, provide the necessary environmental parameter data for calculations of space system performance as modified by the presence of these environmental elements.

Although this standard does not address the effects of human operations or the induced environment that is due to the interaction between the environment and a body in space, this should not be interpreted as indicating that these elements are not important. Their effects on a space system may be greater than that due to the natural environment. These elements vary with human activities, tend to be program peculiar, and, therefore, are simply not appropriate for inclusion in this standard. However, these elements should also be included in the analyses of the effects of the total environment on space systems, to the extent they are applicable.

THIS PAGE INTENTIONALLY LEFT BLANK

CONTENTS

CONTENTS
(continued)

PAGE

CONTENTS
(continued)

PAGE

TABLES



FIGURES

CONTENTS
(continued)

# SECTION 1

# SCOPE

## 1.1 PURPOSE

The purpose and scope of this document is to state the parameters of the earth's natural environment, above 100 kilometers, for use in space vehicle and space system design. The natural environment includes neutral atmosphere, plasma, energetic charged particles, meteoroids, geomagnetic field, electromagnetic radiation, gravitational field, cosmic rays, and solar energetic particles. The geosynchronous environment and the ionosphere are treated in detail. The trapped radiation belts, drag due to the neutral density, atomic oxygen, and particle impacts are treated as well.

## 1.2 APPLICATION

This standard is intended for use in acquisition contracts for selected space vehicles and upper stage vehicles. The standard should be cited in the technical requirements (program-peculiar specifications) as may be appropriate to specify the natural space environment parameters that are applicable for the space system acquisition.

THIS PAGE INTENTIONALLY LEFT BLANK

# SECTION 2

# REFERENCED DOCUMENTS

## 2.1 GOVERNMENT AND NONGOVERNMENT DOCUMENTS

None. All references are listed in Subsection 6.2 instead of this subsection since they are intended only for information and guidance.

## 2*2 ORDER OF PRECEDENCE

In the event of a conflict between the text of this standard and the references cited herein, the text of this standard shall take precedence. However, nothing in this standard shall supersede applicable laws and regulations unless a specific exemption has been obtained.

THIS PAGE INTENTIONALLY LEFT BLANK

# SECTION 3

# DEFINITIONS

Not applicable. A list of definitions is not provided by this standard. The definitions of terms stated in the guidance documents listed for reference in Subsection 6.2 should be used to the extent applicable.

THIS PAGE INTENTIONALLY LEFT BLANK

# SECTION 4

# GENERAL REQUIREMENTS

This standard establishes the time-sensitive and orbit-sensitive parameters for the naturally occuring space environment above 100 kilometers. Space vehicles shall be capable of operating in this naturally occuring environment encountered in orbit (See 6.1). Since not all of the environmental parameters are of concern in all possible orbits, Table I is provided as a guide to identify the usual parameters of concern for generic orbit types.

Space vehicles operating in the space environment experience various effects caused by the vacuum, radiation, and particulate environments, as well as inertial effects. These effects are not specifically addressed in this standard, but shall be included in the analyses of the effects of the environment on the space system, to the extent applicable.

The numerical data presented in Section 5 are current as of the date of issue of this standard. As new data on the space environment are obtained, the models recommended or referenced may be superseded. New models which are intended to supercede the models recommended or referenced in this document may be used as approved substitutes provided they are issued by the same agency or sanctioned by the same authoritative body as the models which they supercede.

TABLE I. Orbit/Environment Concerns

| PARAGRAPH | TOPIC | ORBITS | | | | |
|---|---|---|---|---|---|---|
| | | less than 1000 km | 1000 to 5000 km | greater than 5000 km | Geosync | Polar |
| 5.1.1 | Cosmic Rays | X | X | X | X | X |
| 5.1.2 | Trapped Radiation | X | X | X | X | X |
| 5.1.2.1 | Inner Zone | X | X | X | | X |
| 5.1.2.2 | Slot Region | X | X | X | | X |
| 5.1.2.3 | Outer Zone | | | X | | X |
| 5.1.2.4 | Geosynchronous | | | | X | |
| 5.1.2.5 | Trans-geosynchronous | | | X | X | |
| 5.1.3 | Solar Particles | X | X | X | X | X |
| 5.1.4 | Solar/Magnetic Storm Effects | X | X | X | X | X |
| 5.2.1 | Ionosphere | X | | | | |
| 5.2.2 | Plasmasphere | | X | X | X | X |
| 5.2.3 | Auroral Zone | | | | | X |
| 5.3 | Neutral Atmosphere | X | | | | |
| 5.4 | Meteoroids | X | X | X | X | X |
| 5.5 | Geomagnetic Field | X | X | X | X | X |
| 5.6 | Electromagnetic Radiation | X | X | X | X | X |
| 5.7 | Solar Radiations | X | X | X | X | X |
| 5.8 | Gravitational Field | X | X | X | X | X |

# SECTION 5

# DETAILED REQUIREMENTS

## 5.1 ENERGETIC CHARGED PARTICLES.

Energetic charged particles produce effects in materials primarily through their ionizing action. Effects include radiation damage in electronics, solar cells, and optical materials; electrostatic discharge; backgrounds in sensors; single-event upsets in digital electronics; optical noise; and other deleterious effects.

5.1.1 Cosmic Rays Cosmic rays are highly relativistic charged particles of solar and galactic origin. They are highly ionizing and highly penetrating. The primary concerns with cosmic rays are their background signatures in electronic and optical devices and the single-event upset phenomenon, in which the high density of ionization along a track in an electronic device acts as a signal in that device.

5.1.1.1 Galactic Cosmic Rays For the purposes of this Standard, the cosmic ray environment is defined by Figures 1, 2, 3, and 4, and Table II. Figure 1 presents the differential energy spectra for hydrogen and helium nuclei, which constitute respectively 83 percent and 13 percent of the primary cosmic rays. Figure 2 presents the electron component which constitutes 3 percent of the cosmic rays. Figure 2 is a composite figure, including both galactic and solar electrons. Because of their importance to single-event upset events in microelectronics, the cosmic ray spectrum of iron nuclei is presented in Figure 4. Table II provides the cosmic ray composition for helium plus nuclei up to and including the iron group. The elements above He in the spectrum constitute about 1 percent of the primary cosmic rays. For specific missions where detailed analyses of cosmic ray effects are required, the guidelines, recommendations, and methods of generating appropriate mission-specific environmental models, as described in Refs. 6.2 a, 6.2 b, 6.2 c, and 6.2 d, shall be applicable. The least severe environment under which the space vehicle shall be capable of operating is that associated with the so-called "solar minimum" (see Paragraph 5.1.1.1.1 below). The data for composite particles presented in Figures 1, 2, 3, and 4 are given in terms of differential energy flux (number of particles per unit energy) per nucleon. Protons and electrons (Figures 1 and 3) are not composite particles.

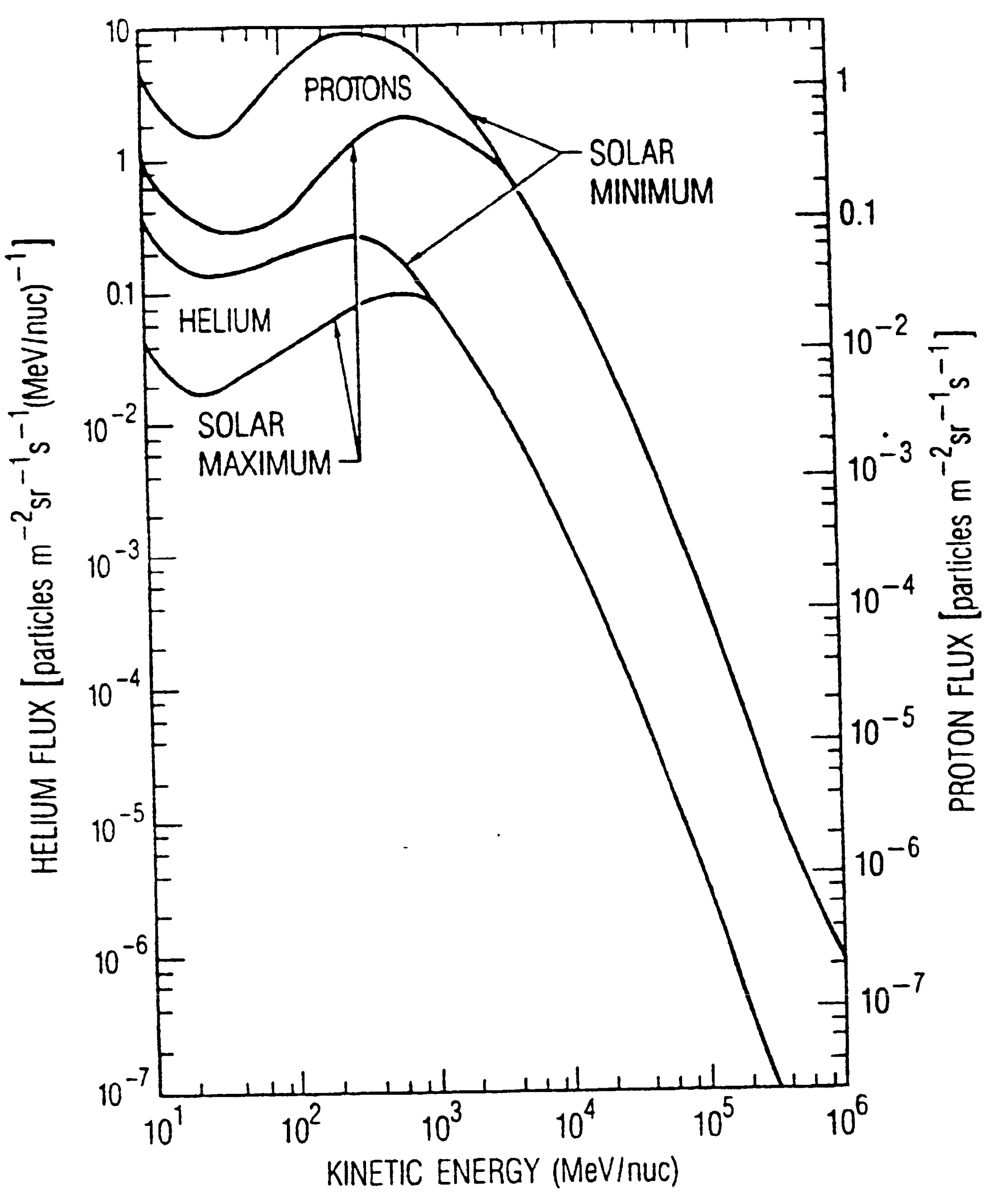


FIGURE 1. Cosmic Ray Differential Energy Spectra for H and He

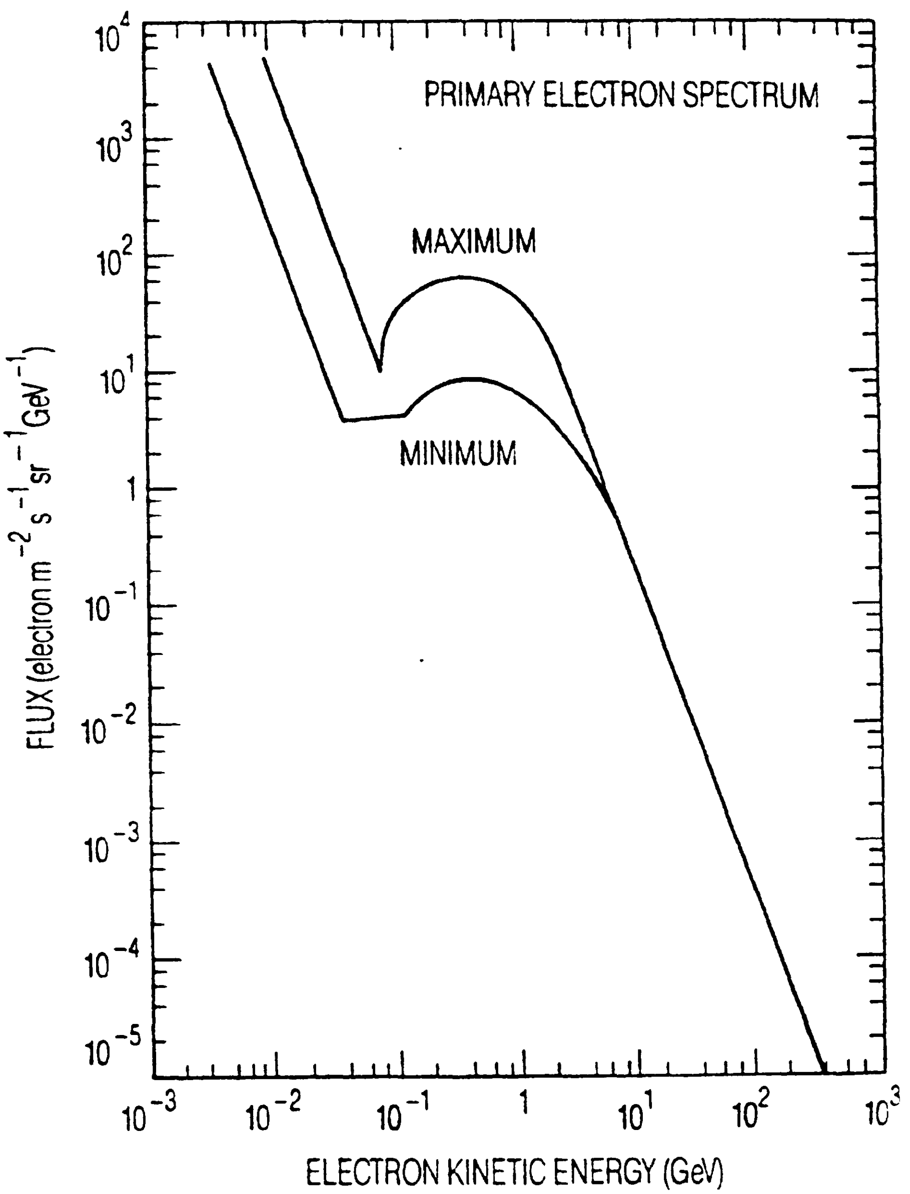


FIGURE 2. Cosmic Ray Differential Energy Spectra for Electrons

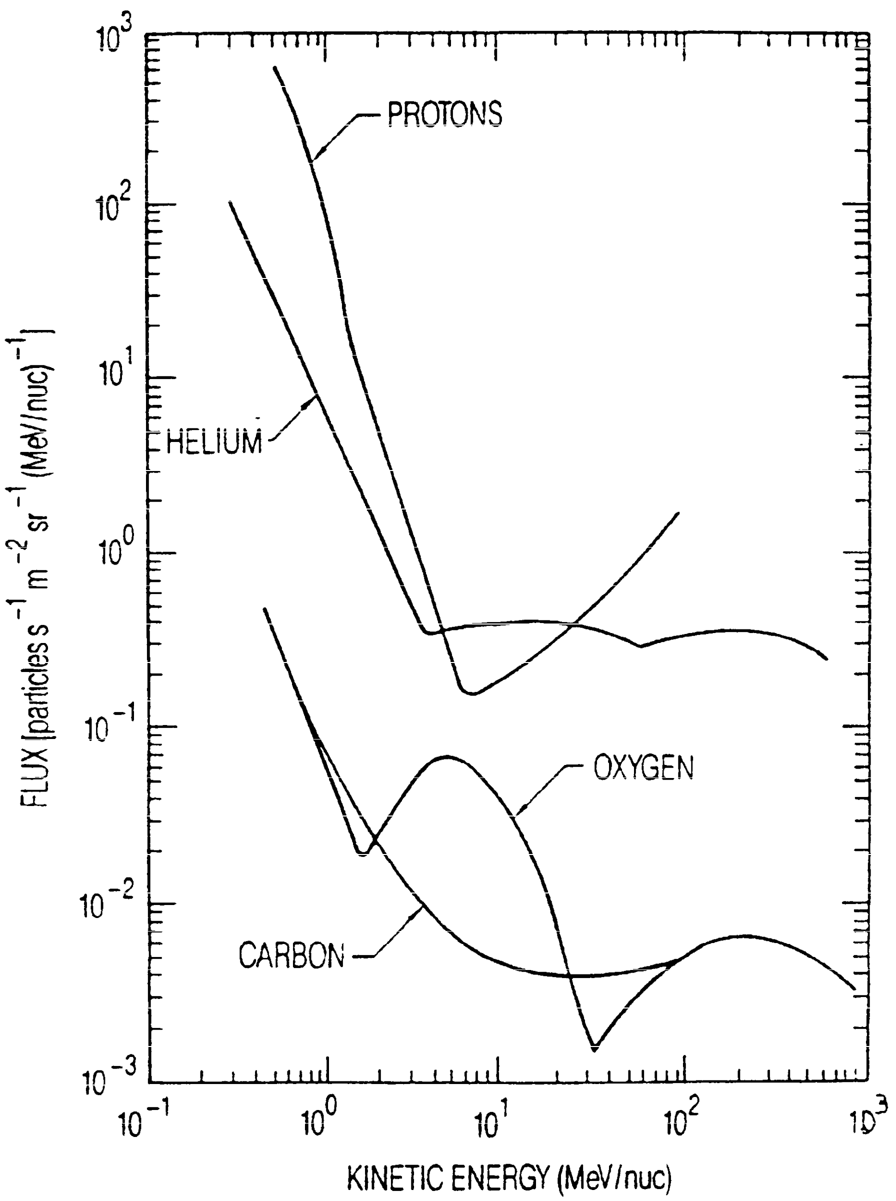


FIGURE 3. Anomalous Component of Cosmic Ray Differential Energy Spectra for H. He. C. & O

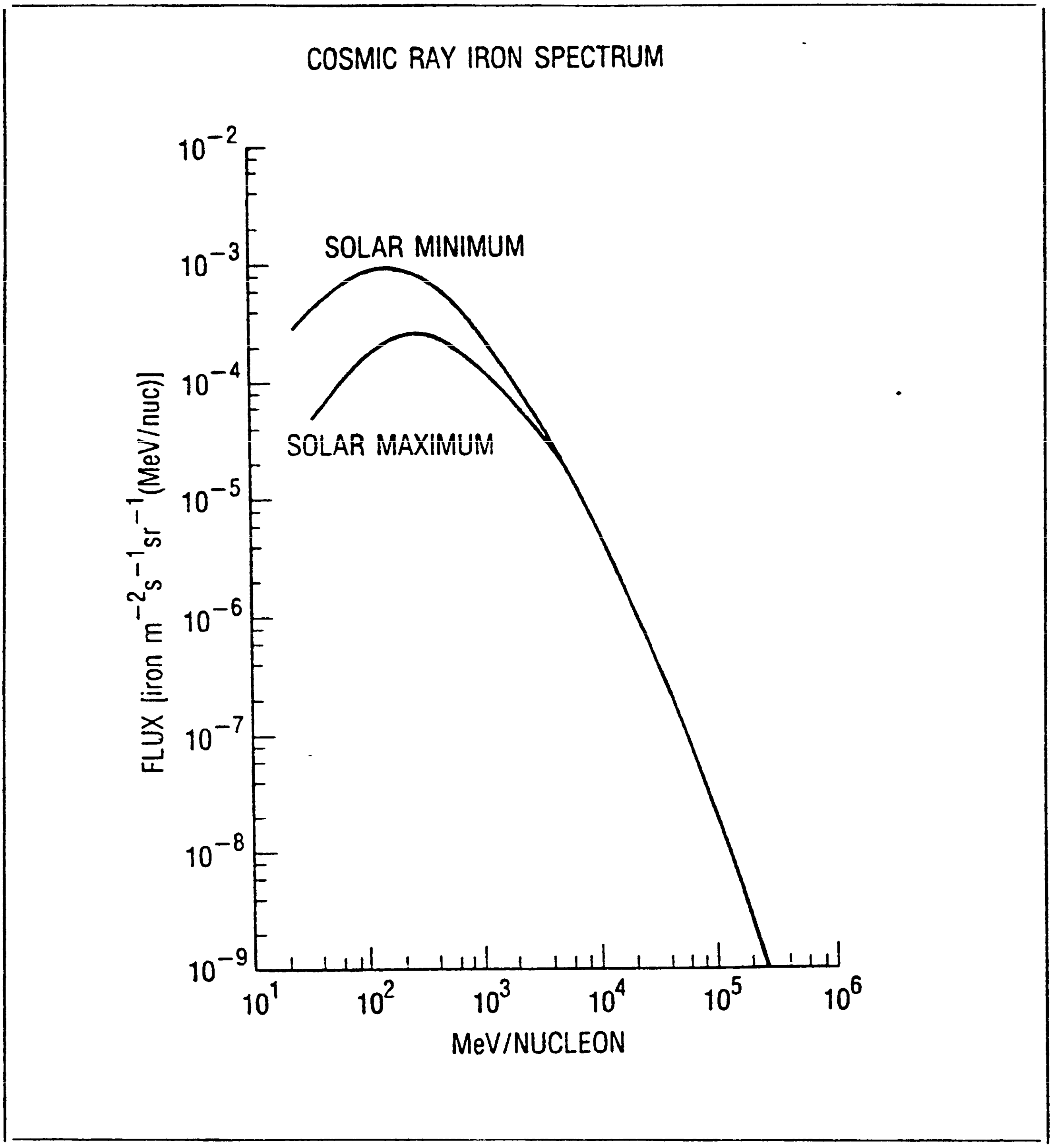


FIGURE 4. Spectrum of Cosmic Ray Iron Nuclei

TABLE II. Heavy Cosmic Ray Abundance

| SPECIES | Relative Abundance Greater than 450 MeV/Nuc |
|---|---|
| He | 44700 ± 500 |
| Li | 192 ± 4 |
| Be | 94 ± 2.5 |
| B | 329 ± 5 |
| C | 1130 ± 12 |
| N | 278 ± 5 |
| O | 1000 |
| F | 24 ± 1.5 |
| Ne | 158 ± 3 |
| Na | 29 ± 1.5 |
| Mg | 203 ± 3 |
| Al | 36 ± 1.5 |
| Si | 141 ± 3 |
| P | 7.5 ± 0.6 |
| S | 34 ± 1.5 |
| Cl | 9.0 ± 0.6 |
| A | 14.2 ± 0.9 |
| K | 10.1 ± 0.7 |
| Ca | 26 ± 1.3 |
| Sc | 6.3 ± 0.6 |
| Ti | 14.4 ± 0.9 |
| V | 9.5 ± 0.7 |
| Cr | 15.1 ± 0.9 |
| Mn | 11.6 ± 1.0 |
| Fe | 103 ± 2.5 |
| Ni | 5.6 ± 0.6 |

5.1.1.1.1.1 Variability of Galactic Cosmic Rays Figures 1, 2, and 3 indicate the variability of the cosmic-ray flux intensity as a function of solar cycle. The intensity of the low energy end of the spectrum undergoes a periodic modulation with the eleven-year sunspot cycle, where the intensity is approximately anti-correlated with the sunspot number and varies in intensity by about a factor of five over the eleven-year cycle. A second variation is the “anomalous component” shown in Figure 3. Enhancements exceeding a factor of ten relative to the carbon flux have been observed in the fluxes of hydrogen, helium, and oxygen ions. The protons in the anomalous component are most intense around 100 MeV. The alpha particle intensity peaks between 10 and 50 MeV/nucleon, and oxygen around 10

MeV/nucleon. Because of the relatively low energy range, atomic number, and overall intensity of the anomalous component constituents, the latter usually are of small significance in the overall environment, but may be significant in special applications. The anomalous component shall be included in the cosmic ray environment which is used to analyze the performance of a space vehicle or space system.

Several other types of temporal variability in the galactic cosmic ray flux have been observed and are described in Ref. 6.2 a. These fluctuations in particle flux occur at energies below 100 MeV/nucleon and are referred to as 'interplanetary weather." Their effect on space vehicles and space systems using current technology is minimal in most cases, but shall be considered in cases where sensitive components are used and extremely high reliability of operation is required. The software in Ref. 6.2 d provides for the effect of this variability on the environmental model by requesting the "interplanetary weather index" value as input.

5.1.1.1.2 Access of Galactic Cosmic Rays. Spatial variation in the particle flux intensities within the magnetosphere occur because of the Earth's magnetic field and physical shadow at low altitude. Where necessary, the primary environments specified in Paragraph 5.1.1.1 can be modified by incorporating geomagnetic cutoff rigidities and the effect of Earth's shadow in the model. Provision for calculating these effects has been made in the CREME computer software of Ref. 6.2 d.

5.1.1.2 Solar Cosmic Rays. Solar cosmic rays are present in space about two percent of the time. The solar cosmic ray component of the environment can be ignored in analyses only if disruption of space vehicle or space system operation more than two percent of the time can be tolerated (see Paragraph 5.1.1.2.1 below), and total accumulated dose below about 100 krads (Si) is of no concern. Otherwise, the recommendations and methods contained in Ref. 6.2 a, 6.2 b, 6.2 c, and 6.2 d shall be followed. Attention should be paid to the question of survival during at least one large flare, as defined by Ref. 6.2 a. See also Paragraph 5.1.3.

5.1.1.2.1 Variability of Solar Cosmic Rays. Major solar flares are characterized by a random frequency distribution, modulated by the eleven-year sunspot cycle. Near the peak of the cycle, major flares occur at the rate of several per year, while during "solar minimum" the rate drops to less than one per year. The particle fluxes associated with individual flares last anywhere from two hours to several days, and vary from flare to flare by several orders of magnitude. Large flare-to-flare variations in particle composition (especially in the ratio of protons to heavier ions) are also observed. On the average, cosmic ray particle environments enhanced by solar flares are encountered about two percent of the time. All considerations of particle access to regions within the magnetosphere discussed in paragraph 5.1.1.1.2 apply here. As a minimum, space vehicles operating in polar or geosynchronous and trans-geosynchronous orbits shall be capable of operating normally in the solar particle environment enhancements listed in Paragraphs 5.1.3.1 and 5.1.3.2.

5.1.2 Trapped Radiation Belts. The Earth's magnetic field contains large fluxes of energetic-particles including electrons with energies in excess of 5 MeV, protons with energies in excess of 400 MeV, and energetic higher-Z ions (Z is the atomic number). The source of these particles is in-situ acceleration of lower energy particles by magnetic storms, trapping of decay products of energetic neutrons produced in the upper atmosphere by collisions of cosmic rays with atmospheric nuclei, and in some instances by trapping of solar flare particles. The magnetospheric energetic particle population is normally categorized by region and species. Large magnetic storms, with a Dst (an index which is a world-wide average of the change in the low-latitude horizontal component of the Earth's magnetic field, in nanoteslas) of -200 nanoteslas or more, produce major perturbations in the magnetospherically trapped fluxes. Smaller storms, with Dst of approximately -50 nanoteslas, produce substantially smaller, though significant, perturbations (see Paragraph 5.1.4). For the purpose of defining the various regions of the magnetosphere which contain significant trapped fluxes of energetic particles, a two-parameter description of the geomagnetic field is used, B and L, where B is the field intensity and L is McIlwain's parameter (Ref. 6.2 e). In a dipole field, the value of L corresponds to the radial distance in units of earth radii from the center of the Earth to the equatorial crossing of the field line labeled "L".

The intensity numbers given in Paragraph 5.1.2 all refer to the highest intensity that may be encountered in the region defined within a given paragraph. Changes in the design of the radiation resistance of satellites should not be made solely on the basis of the numbers listed in Paragraph 5.1.2. If the listed values exceed the survival capability of a system in that particular orbit, more precise calculations should be made using the referenced NASA particle models before any changes in system design are made to provide survival margin. Where two models are listed, MAX and MIN, the electron MAX model is more severe than the MIN model because magnetic storms during solar maximum add energetic electrons to the magnetosphere. For energetic protons, the MIN model is more severe because during solar minimum the atmospheric scale height is smaller and fewer energetic protons are removed by the residual atmosphere.

5.1.2.1 Inner zone. For the purpose of defining the inner radiation zone for this Standard, the region from 100 kilometers altitude to an upper limit of L = 2 shall be used, where L is McIlwain's parameter and corresponds to a dipole magnetic field line which crosses the equator at a geocentric distance of two earth radii (Re). For a dipole field, this field line crosses the equator at about 6400 kilometers altitude and intersects the surface of the Earth at a latitude of about 45 degrees. Intensity numbers in this section may be reduced to 20 percent of the listed value for satellites with apogees below 1000 km. For low altitude polar orbits, also see paragraph 5.2.3.

5.1.2.1.1 Protons. Vehicles traversing the inner radiation zone shall be capable of operating in a penetrating proton environment with maximum average omnidirectional fluxes of:

a. $4 \times 10^7$ protons per square centimeter per second above 0.1 MeV ($p/cm^2$-sec or p $cm^{-2}$ $sec^{-1}$)

b. $1 \times 10^7$ $p/cm^2$-sec above 1 MeV

c. $5 \times 10^5$ $p/cm^2$-sec above 10 MeV

d. $2 \times 10^4$ $p/cm^2$-sec above 100 MeV, and of

e. $8 \times 10^2$ $p/cm^2$-sec above 400 MeV

For the purposes of calculating radiation dose or instantaneous interference levels in devices due to the inner zone protons, the AP8MIN model shall be used (Ref. 6.2 f).

5.1.2.1.1.1 Proton Variability. The energetic protons in the inner zone are only slightly and slowly affected by atmospheric density variations as a function of solar cycle and by the secular variations of the Earth's magnetic field. For the purposes of this Standard, other than long-term planning, the inner-zone proton population may be considered static. For long term planning, the effect of the secular variation of the Earth's magnetic field shall be included in the high-energy proton environment (Ref. 6.2 g).

5.1.2.1.2 Electrons. Vehicles traversing the inner radiation zone shall be capable of operating in an electron environment with maximum average omnidirectional fluxes of:

a. $2.3 \times 10^8$ $e/cm^2$-sec above 0.1 MeV

b. $1 \times 10^7$ $e/cm^2$-sec above 0.5 MeV, and of

c. $1 \times 10^5$ $e/cm^2$–sec above 2 MeV

For the purposes of calculating radiation dose or instantaneous interference levels in devices due to the inner zone electrons, the AE–6 (maximum) model shall be used (Ref. 6.2 h).

5.1.2.1.2.1 Electron Variability At L values below 1.7, the electron environment can be considered to be static. Electrons in the inner zone between L = 1.7 and L = 2 are subject to increases of several orders-of-magnitude at times of magnetic storms. The increases decay exponentially with time constants of a few days to a few weeks. At peak, these increases do not exceed the limits given above in Paragraph 5.1.2.1.2 and may be ignored for the purposes of this Standard.

5.1.2.2 Slot Region. For the purpose of defining the slot region of the magnetospheric radiation zones in this Standard, lower and upper limits of L = 2 and L = 2.8, respectively, shall be used, where L is McIlwain's parameter (see paragraph 5.1.2.1 above) . For a dipole field, the field lines defined by L = 2 and L = 2.8 cross the equator at altitudes of about 6400 and 11500 kilometers, and intersect the surface of the Earth at latitudes of about 45 degrees and 53.3 degrees, respectively.

5.1.2.2.1 Protons. Vehicles traversing the slot region of the magnetosphere shall be capable of operating in a penetrating proton environment with maximum average omnidirectional fluxes of:

a. $3x10^8$ p/$cm^2$–sec above 0.1 MeV

b. $6x10^7$ p/$cm^2$–sec above 1 MeV

c. $2x10^5$ p/$cm^2$–sec above 10 MeV, and of

d. $7x10^3$ p/$Cm^2$-sec above 100 MeV

For the purposes of calculating radiation dose or instantaneous interference levels in devices due to the slot protons, the AP8MIN model shall be used (Ref. 6.2 f).

5.1.2.2.1.1 Proton Variability For the purpose of this Standard, the proton fluxes in the slot region with energies below 10 MeV shall be assumed to have a short-term increase of an order-of-magnitude after major magnetic storms, with exponential decay times of several days. The fluxes of protons with energies above 10 MeV shall be assumed to be static.

5.1.2.2.2 Electrons. Vehicles traversing the slot region of the magnetosphere shall be capable of operating in an electron environment with maximum average omnidirectional fluxes of:

a. $3x10^8$ e/$cm^2$-sec above 0.1 MeV

b. $1x10^7$ e/cm$^2$-sec above 0.5 MeV, and of

c. $1x10^4$ e/cm$^2$-sec above 2 MeV

For the purposes of calculating radiation dose or instantaneous interference levels in devices due to the slot electrons, the AE-6 (maximum) model shall be used (Ref. 6.2 h).

5.1.2.2.2.1 Electron Variability Lower-energy electrons in the slot region show great variability in intensity in response to major magnetic storms, with as great as five orders-of-magnitude increase at 0.7 MeV in a 4-day period having been observed. For the purposes of this Standard, instantaneous fluxes between 0.1 and 0.5 MeV may be assumed to increase to $3x10^9$ e/cm$^2$-sec above 0.1 MeV and to $1x10^8$ e/cm$^2$-sec above 0.5 MeV.

5.1.2.3 Outer Zone. For the purpose of defining the outer radiation zone in this Standard, lower and upper limits of L = 2.8 and L = 6.6 shall be used, where L is McIlwain's parameter (see Paragraph 5.1.2.1 above). For a dipole field, the field lines defined by L = 2.8 and L = 6.6 cross the equator at altitudes of about 11500 and 35700 kilometers, and intersect the surface of the Earth at latitudes of about 53.3 degrees and 67.1 degrees, respectively.

5.1.2.3.1 Protons. Vehicles traversing the outer zone region of the magnetosphere shall be capable of operating in a penetrating-proton environment with maximum average omnidirectional fluxes of:

a. $4x10^8$ p/cm$^2$-sec above 0.1 MeV

b. $4x10^7$ p/cm$^2$-sec above 1 MeV

c. $1x10^4$ p/cm$^2$-sec above 10 MeV. and of

d. $1x10^2$ p/cm$^2$-sec above 20 MeV

For the purposes of calculating radiation dose or instantaneous interference levels in devices due to the outer zone protons, the AP8MIN model shall be used (Ref. 6.2 f).

5.1.2.3.1.1 Proton Variability. For the purpose of this Standard, the proton fluxes in the outer zone with energies below 10 MeV shall be assumed to have a short-term increase of an order-of-magnitude after major magnetic storms, with exponential decay times of several days. The fluxes of protons with energies above 10 MeV shall be assumed to be static.

5.1.2.3.2 Electrons. Vehicles traversing the outer zone region of the magnetosphere shall be capable of operating in an electron environment with maximum average omnidirectional ‘fluxes of:

a. $4x10^7$ e/cm$^2$-sec above 0.1 MeV

b. $1x10^7$ e/cm$^2$–sec above 0.5 MeV, and of

c. $1x10^6$ e/cm2-sec above 2 MeV

For the purposes of calculating radiation dose or instantaneous interference levels in devices due to the outer-zone electrons, the AE-8 model (Ref. 6.2 i) shall be used.

5.1.2.3.2.1 Electron Variability High-energy electrons in the outer-zone region of the magnetosphere show great variability in intensity in response to major magnetic storms, with as great as 4 orders-of-magnitude increases at 1.5 MeV in a l-day period having been observed. For the purposes of this Standard, instantaneous omnidirectional fluxes may be assumed to increase to:

a. $6x10^8$ e/cm$^2$-sec above 0.5 MeV

b. $1x10^8$ e/cm$^2$–sec above 1 MeV, and to

c. $4x10^6$ e/cm$^2$–sec above 2 MeV

5.1.2.3.3 Higher-Z Particles. Higher-Z particles, particularly He and O ions, are trapped in the Earth’s magnetosphere, predominantly near the geomagnetic equator. At a given energy, He ions can be assumed to be 3 orders-of-magnitude less intense than the protons, and the O ions can be assumed to be 2 orders–of–magnitude less intense than the He ions. See Paragraph 5.1.3.3.

5.1.2.3.3.1 Higher-Z Particle Variability. Little is known about the variability of higher–Z particles in the outer zone other than the fact that major magnetic storms transport many of them to lower positions on the field line, producing temporary increases in the lower–altitude fluxes. For the purposes of this Standard, the higher–Z fluxes may be assumed to be static.

5.1.2.4 Geosynchronous Orbit. The geosynchronous orbit is that orbit that has a period which is the same as the rotation period of the Earth and with a near-zero inclination. For the purpose of defining the radiation environment of the geosynchronous orbit region, L = 6.6 shall be used, where L is McIlwain’s parameter (see Paragraph 5.1.2.1 above). For a dipole field, the field line defined by L = 6.6 crosses the equator at an altitude of about 35700 kilometers and intersects the surface of the Earth at a latitude of about 67.1 degrees.

5.1.2.4.1 Protons. Vehicles in geosynchronous orbit shall be capable of operating in a penetrating-proton environment with maximum average omnidirectional fluxes of:

a. $1x10^7$ p/cm$^2$-sec above 0.1 MeV, and of

b. $1x10^3$ p/cm$^2$-sec above 1 MeV

For the purposes of calculating radiation dose or instantaneous interference levels in devices due to the geosynchronous orbit protons, the AP8MIN model shall be used (Ref. 6.2 f).

5.1.2.4.1.1 Proton Variability For the purpose of this Standard, the proton fluxes in the geosynchronous orbit region shall be assumed to have a short-term increase of an order-of-magnitude after major magnetic storms, with exponential decay times of several days. The fluxes of protons with energies above 10 MeV shall be assumed to be static with the exception of solar flare injection of protons into the geosynchronous region. For solar flare injections, see Paragraph 5.1.3.

5.1.2.4.2 Electrons. Vehicles in geosynchronous orbit shall be capable of operating in an electron environment with average omnidirectional fluxes of:

a. $2x10^7$ e/cm$^2$-sec above 0.1 MeV

b. $8x10^6$ e/cm$^2$-sec above 0.5 MeV

c. $2x10^6$ e/cm$^2$-sec above 1 MeV, and of

d. $2x10^4$ e/cm$^2$-sec above 2 MeV

For the purposes of calculating radiation dose or instantaneous interference levels in devices due to the geosynchronous orbit electrons, the AE-8 model shall be used (Ref. 6.2 j).

5.1.2.4.2.1 Electron Variability During and for several days after a major magnetic storm, electron fluxes in the geosynchronous region will be assumed to increase by an order-of-magnitude above the average flux level given in Paragraph 5.1.2.4.2.

5.1.2.5 Trans-geosynchronous Orbits. For the purpose of defining the trans-geosynchronous radiation zone in this Standard, lower and upper limits of L = 6.6 and L = 10 shall be used, where L is McIlwain's parameter (see Paragraph 5.1.2.1 above). For a dipole field, the field lines defined by L = 6.6 and L = 10 cross the equator at altitudes of about 35700 and 57300 kilometers, and intersect the surface of the Earth at latitudes of about 67.1 degrees and 71.6 degrees, respectively.

5.1.2 .5.1 Protons. Vehicles traversing the trans-geosynchronous region of the magnetosphere shall be capable of operating in a proton environment with maximum average - omnidirectional fluxes of:

a. $1x10^7$ p/$cm^2$-sec above 0.1 MeV, and of

b. $1x10^3$ p/$cm^2$-sec above 1 MeV

For the purposes of this Standard, protons with energies above 10 MeV can be ignored except for injections of solar-flare protons (see Paragraph 5.1.3). For the purposes of calculating radiation dose or instantaneous interference levels in devices due to the trans-geosynchronous protons, the AP8MIN model shall be used (Ref. 6.2 f).

5.1.2.5.1.1 Proton Variability For the purpose of this Standard, the proton fluxes in the trans-geosynchronous region with energies below 10 MeV shall be assumed to have a short-term increase of an order-of-magnitude during major magnetic storms and substorms, with exponential decay times of several hours. The fluxes of protons with energies above 10 MeV shall be assumed to be produced only during solar flare events (see Paragraph 5.1.3).

5.1.2.5.2 Electrons. Vehicles traversing the trans-geosynchronous region of the magnetosphere shall be capable of operating in an electron environment with maximum average omnidirectional fluxes of:

a. $2x10^7$ e/$cm^2$-sec above 0.1 MeV

b. $8x10^6$ e/$cm^2$-sec above 0.5 MeV

c. $2x10^6$ e/$cm^2$-sec above 1 MeV, and of

d. $1x10^4$ e/$cm^2$-sec above 2 MeV

For the purposes of calculating radiation dose or instantaneous interference levels in devices due to the trans-geosynchronous electrons, the AE-8 model shall be used (Ref. 6.2 i).

5.1.2.5.2.1 Electron Variability. High-energy electrons in the trans-geosynchronous region of the magnetosphere show great variability in intensity in response to magnetic storms and substorms. For the purposes of this Standard, instantaneous omnidirectional fluxes may be assumed to increase by one order-of-magnitude above the averages given in Paragraph 5.1.2.5.2 during magnetic storms and substorms

5.1.2.5.3 Higher-Z Particles. For the purposes of this Standard, higher-Z particles may be considered to be absent from the trans-geosynchronous region except for cosmic rays and solar–flare particles (see Paragraphs 5.1.1 and 5.1.3.).

5.1.3 Solar Particles At times, solar flares eject coronal matter at very high velocities in large quantities. This matter consists primarily of ionized hydrogen, helium, and electrons. The geomagnetic field prevents most of these particles from entering the near-earth region except for the polar region, the trans-geosynchronous region, and, for energetic protons, the geosynchronous region. These fluxes persist for a period of a few days after a major solar flare. Solar flares which produce energetic particles are most prevalent near and just after the solar sunspot maximum.

5.1.3.1 Electrons. Electrons appear over the polar caps after major solar flares, but the fluxes are negligible compared to the proton fluxes. These fluxes are isotropic except for the solid angle represented by the downward-looking atmospheric loss cone (the portion of the distribution that would mirror within the atmosphere) . Electron spectra are soft, with typical energy spectra of the form $NE = NoE^{-k}$, where No is typically less than $10^3$ e/cm$^2$-sec-steradian, E is in units of MeV, and k is between 2 and 3. The intensities usually persist for a few days.

5.1.3.2 Protons. The typical fluence of energetic solar flare protons in the near-earth region is $2x10^7$/cm$^3$ per year above 30 MeV. Over a 10-year period, the average annual fluence above 30 MeV is $4.8x10^8$/cm$^2$. During a typical solar cycle, 90 percent of the fluence is due to a single large event which persists for a few–day period. Polar–orbiting, geosynchronous, and trans-geosynchronous orbit satellites may experience, and shall be expected to survive, one large event with the following omnidirectional integral fluences:

a. $2x10^{10}$ greater than 10 MeV

b. $5x10^9$ greater than 30 MeV

c. $2x10^9$ greater than 60 MeV, and

d. $5x10^8$ greater than 100 MeV

These numbers are representative of the October 1989 solar flare.

5.1.3.3 Higher–Z Particles. Solar flare events include some higher-Z (Z greater than 2) particles. These higher-Z particles, while of concern to lightly shielded electronic components on interplanetary missions, may be neglected in comparison to the natural flux of galactic cosmic ray high–Z fluxes.

5.1.4 Solar/Magnetic Storm Effects Solar flares, high speed solar wind streams from coronal holes (regions on the sun which look dark because they are cooler than the surrounding areas), and solar magnetic field polarity reversals embedded in the normal solar wind all produce geomagnetic storms. These storms accelerate energetic particles in the magnetic field. They also precipitate some energetic particles into the atmosphere. Averaged over a solar cycle, major magnetic storms (producing major effects in the trapped particle populations) occur about once per year and minor magnetic storms occur about twice per year. These storms peak at, and following, the sunspot maximum. The flux numbers provided in Paragraph 5.1.2 include these storm effects.

For space vehicles or space systems which are sensitive to the flux peaks, major magnetic storms shall be assumed to occur once per year during the five year period around the sunspot minimum and twice per year during the remainder of the sunspot cycle. Minor magnetic storms shall be assumed to occur with twice that frequency.

## 5.2 PLASMA ENVIRONMENT

The plasma environment in the magnetosphere includes the ionosphere and the plasmasphere. The ionosphere is typically considered to be the region from about 80 km to about 1000 km altitude and is a transition region from a relatively un-ionized atmosphere to a fully ionized plasmasphere. The plasmasphere typically contains ion densities of the order of $10^4/cm^3$ to $10^5/cm3$ at 1000 km and diminishes to about $10^3/cm^3$ around 12000 to 15000 km at the equator. At higher latitudes, this dropoff in density occurs at lower altitudes, approximately following the magnetic field line configuration. This region is bounded by the plasmapause, a boundary where a sharp drop of a factor of 30 to 100 in ion density occurs. The ion composition is altitude dependent, with 0+, $O_2^+$, and $NO^+$ being major constituents below 300 km; $0^+$ and $H^+$ the primary constituents between 300 and 1000 km; and $H^+$ and $He^+$ the primary constituents above 1200 km. The ionospheric reference models contain composition information. In the auroral zone, acceleration and ionization processes produce bands of enhanced ion density aligned along contours of magnetic latitude. Densities can exceed $10^6/cm^3$ with energies of tens of volts. Within an auroral form, maximum plasma energies of several hundred volts may be encountered. See Paragraph 5.2.3.

5.2.1 Ionosphere. A smooth, undisturbed ionosphere can degrade low frequency (less than 300 MHz) space-to-ground communications links and signals from space-based radars. Ionospheric impacts on wave propagation include radio-wave absorption, signal-time delay, polarization rotation, Doppler shift, refraction, “ and radar-pulse distortion.

The electron concentration is essentially equal to the ion concentration everywhere in the ionosphere. The only exception occurs during the daytime at altitudes below about 80 km, where electrons may combine with molecules to form negative ions. Solar radiation is principally responsible for the daytime ionosphere, although particle precipitation at auroral and midlatitude regions may serve to augment plasma concentrations. Because of the solar control, the ionosphere exhibits diurnal, seasonal, and solar cycle variations. Representative examples of ionospheric electron concentration profiles are presented in Figure 5 for daytime and nighttime conditions at the minimum and maximum of the solar cycle.

The ionospheric profiles of Figure 5 are averaged over the seasons. The nighttime F-layer tends to be at higher heights in the summer than in the winter, the tendency being accentuated at lower latitudes. In general, the nighttime F-region tends to be thicker when higher. During the daytime, the electron concentration at the F-region peak is considerably larger in winter than in summer; this effect is more evident at high latitudes than at low latitudes. Noontime electron concentration profiles are shown in Figure 6 for summer and winter conditions at three levels of solar activity.

5.2.1.1 Ionospheric Models. Several empirical models are available which furnish a statistically averaged ionosphere at a given location, local time, and month for a specified level of solar activity. The primary model to be used is the International Reference Ionosphere (Refs. 6.2 k and 6.2 1).

Representative results from the International Reference Ionosphere model are presented in Figures 7, 8, 9, and 10, calculated for a solar active period (sunspot number of 70) for January at a longitude and latitude of O degrees. Figure 7 provides a nominal electron number density as a function of altitude for noon and midnight meridians. Figures 8 and 9 provide a comparison of the ion temperatures, $T_i$, and electron temperatures, $T_e$, for noon and midnight from the same source. Figure 10 provides a similar comparison of ion composition.

5.2.1.2 Ionospheric Irregularities Irregularities in ionospheric electron density cause signals transiting the ionosphere to fluctuate in phase and amplitude. This effect is referred to as scintillation. The parameters which serve to characterize a scintillating signal include the signal decorrelation time (t), the frequency selective bandwidth ($f_0$), and the so-called $S_4$ index.

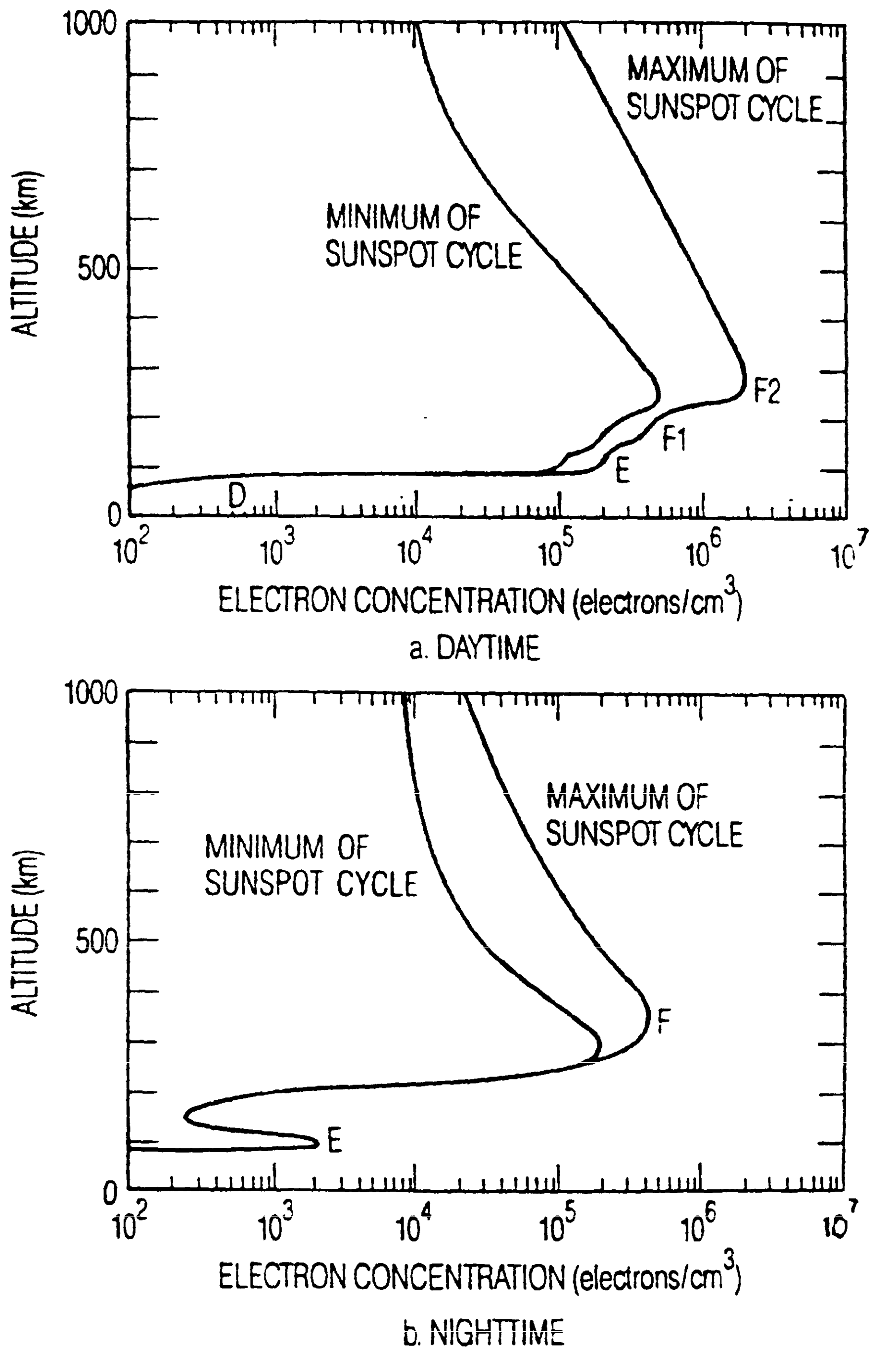


FIGURE 5. Season-Averaged Ionospheric Electron Concentration

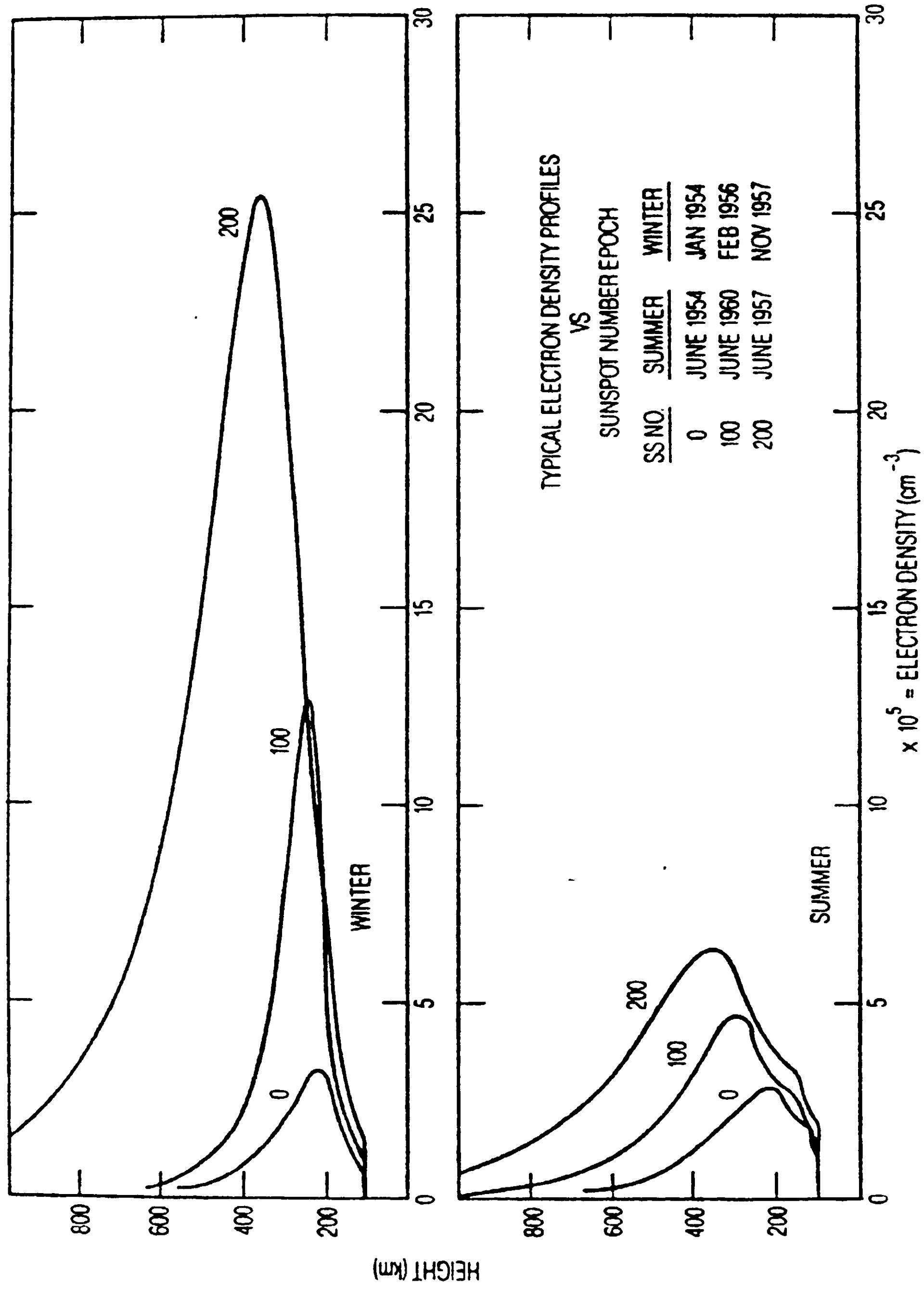


**FIGURE 6.** <u>**Solar-Cycle Effects on the Noon Meridian Ionospheric Electron Concentration**</u>

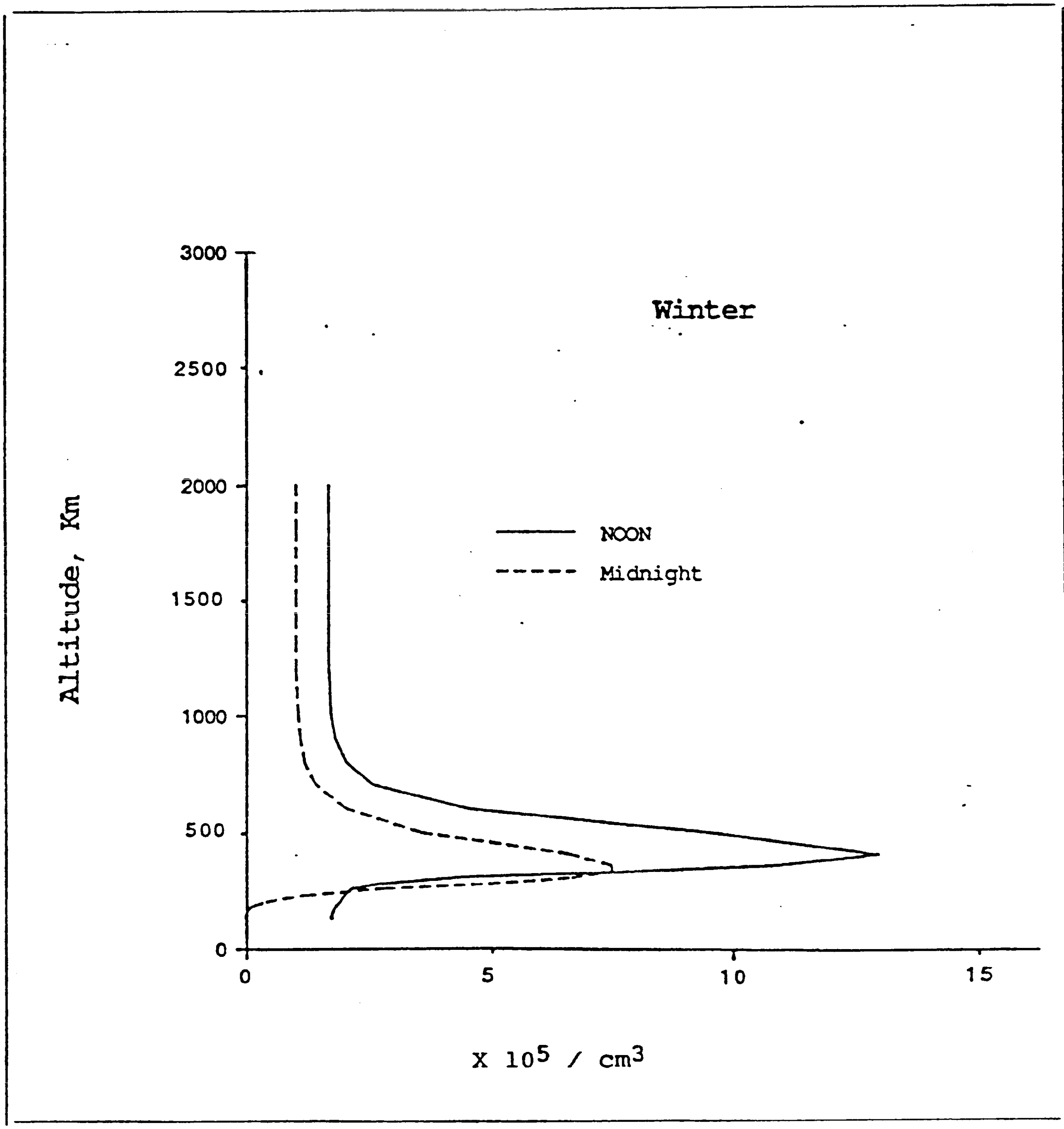


FIGURE 7. Nominal Electron Number Density Profiles Derived from the International Reference Ionosphere

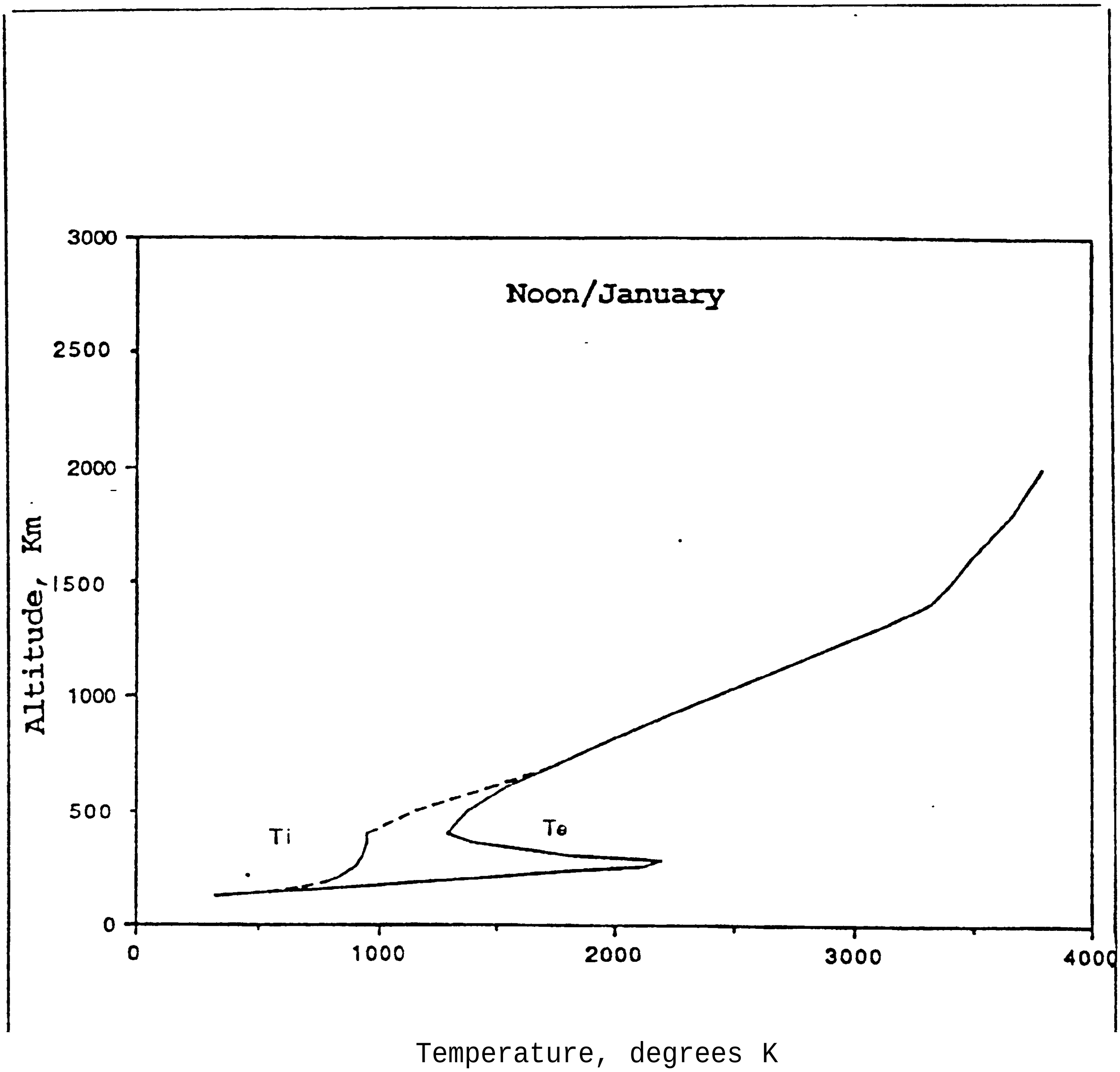


FIGURE 8. Ion and Electron Temperatures Derived from the International Reference IonoSphere Model

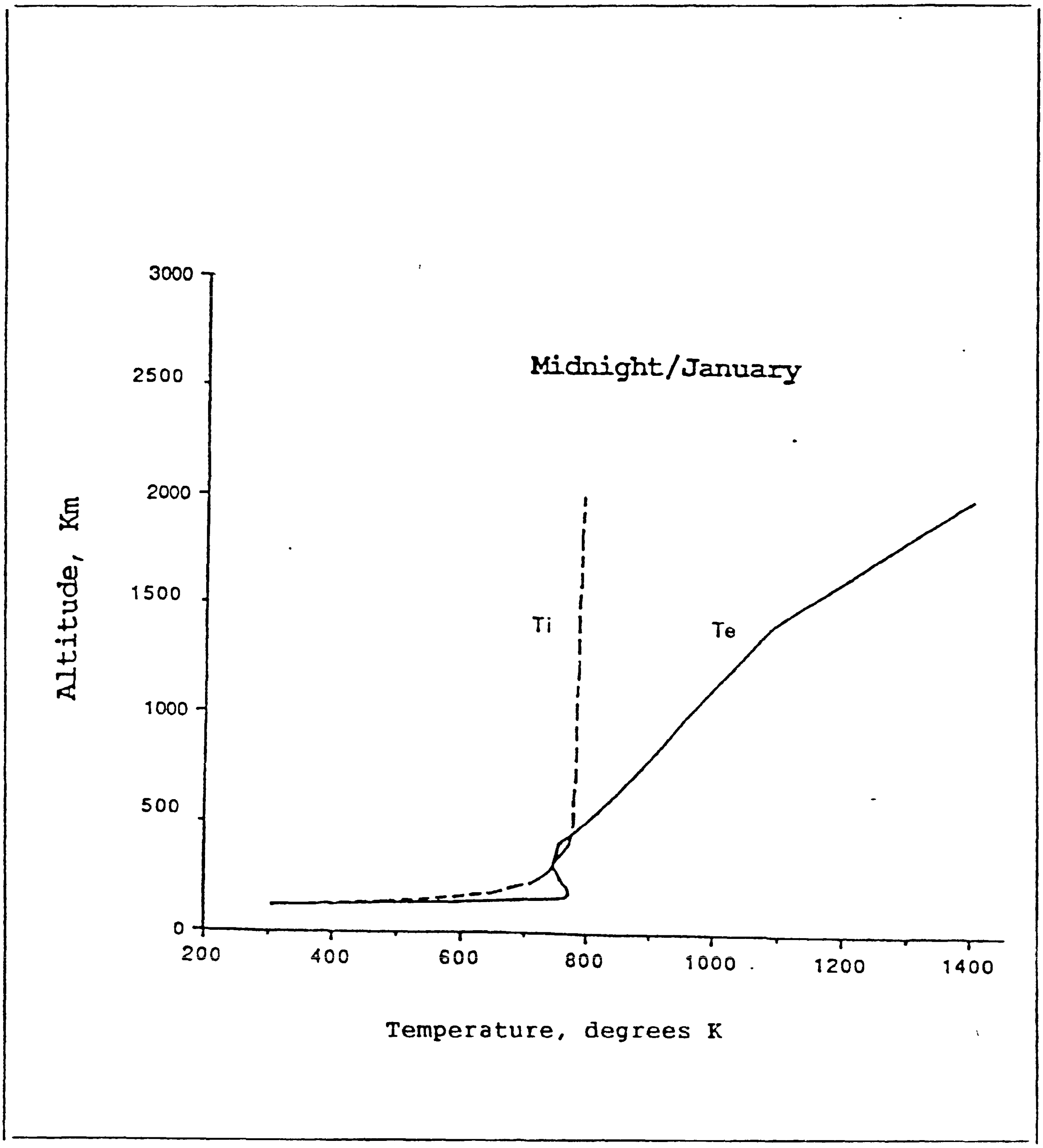


FIGURE 9. Ion and Electron Temperatures Derived from the International Reference Ionosphere Model

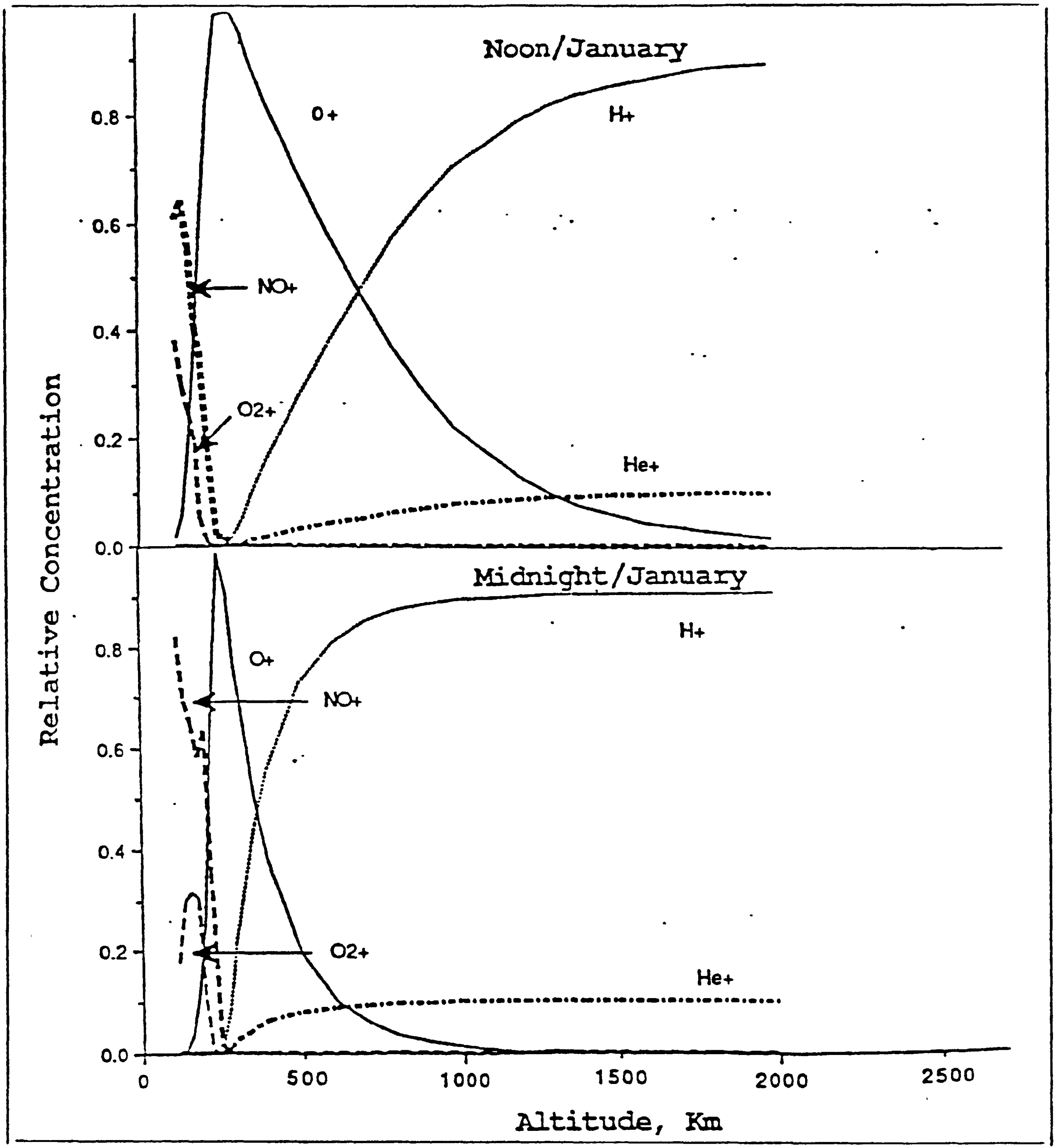


FIGURE 10. Ion Composition Comparisons Derived from the International Reference Ionosphere Model

The $S_4$ index is a measure of the scintillation depth in received signal power. It is defined as:

$$(S_4)^2 = \frac{(\overline{R^4}) - (\overline{R^2})^2}{(\overline{R^2})^2}$$

where R is the amplitude of the wave and a horizontal bar denotes the mean value of the quantity below it.

In Table III, estimates of reasonable worst case values of the $S_4$ index, signal decorrelation time, and frequency selective bandwidth are listed for VHF (approximately 150 MHz) signals propagating through the ionosphere. Also included are ionospheric absorption losses, which are generally very small. At equatorial latitudes, signal scintillation at VHF can be severe ($S_4 = 1$), giving rise to intense Rayleigh fading. This situation is worst during the maximum of the solar sunspot cycle. At solar maximum, $S_4 = 1$ conditions may occur for four hours each night (nominally between 2100 and 0100 local time), a few days a week for approximately six months a year. The particular six months of the year affected is dependent upon geomagnetic longitude. At high latitudes and midlatitudes the scintillations are weaker, and Rayleigh fading is not typically encountered.

TABLE III. Worst-case Signal Propagation Parameters (Scintillation Parameters in the Natural Ionosphere at VHF) (Approximately 150 MHz)

| | $S_4$ | $\tau$ | $f_o$ | Absorption |
|---|---|---|---|---|
| Equatorial | 1* | 0.5-0.05 sec | 80-1 MHz | below 0.5 dB |
| Midlatitudes | 0.2 | several seconds | *** | negligible |
| Auroral | 0.5** | 2.0-0.2 sec | *** | negligible |

* 4 hours per night, a few days per week, 6 months per year

** 4 hours per night

*** Not limited by scintillation

Except for the equatorial $S_4$ index, the VHF results of Table III can be scaled to higher frequencies using the relations $\tau$ approximately equal to $f_r$, $f_0$ approximately equal to $(f_r)^4$ (e.g., Ref. 6.2 m), and $S_4$ approximately equal to $(f_r)^{-1.4}$ for $S_4$ less than 0.7 (Ref. 6.2 n), where $f_r$ is radio wave frequency. In the equatorial region, the condition $S_4 = 1$ occurs less frequently at higher frequencies. At L-band (1.2 GHz), $S_4 = 1$ conditions may occur half as often as at VHF, and at C-band (4 MHz) this condition is fairly rare.

5.2.2 Plasmasphere/Space Plasma. These subparagraphs pertains to all orbits above 1000 km.

5.2.2.1 High-Altitude and Mid- to High-Inclination Orbits The hot plasma electron and ion (proton) components in the near geosynchronous orbits and high-altitude (greater than 25000 km) orbits, mid- to high-inclination orbits, and in the polar auroral zones above approximately 150 km altitude can be represented, as a worst case, by the two-maxwellian function:

$$f(v) = n_1[m/(2\pi kT_1)]^{3/2} \exp(-mv^2/2kT_1) + n_2[m/(2\pi kT_2)]^{3/2} \exp(-mv^2/2kT_2)$$

where: kT is in KeV
$m = 9.11 \times 10^{-28}$ gms for electrons and
$m = 1.67 \times 10^{-24}$ gms for protons

$mv^2/2$ is the particle kinetic energy in KeV

f(v) is the particle distribution function in units of $sec^3\ cm^{-6}$

$n_1$, $kT_1$, $n_2$, and $kT_2$ are defined in Table IV for both electrons and ions.

TABLE IV. Two Maxwellian Fit Parameters

| | $n_1$ ($cm^{-3}$) | $n_2$ ($cm^{-3}$) | $kT_1$ (KeV) | $kT_2$ (KeV) |
|---|---|---|---|---|
| ELECTRONS | 2.67 | 0.625 | 3.1 | 25.1 |
| PROTONS | 0.6 | 1.2 | 0.2 | 28.0 |

A plot of the electron velocity distribution function $f_e(v)$ is given in Figure 11. The electrons are emphasized because they control the potentials of the materials and can penetrate into the materials causing a bulk charge build up. For a more detailed description see Ref. 6.2 0.

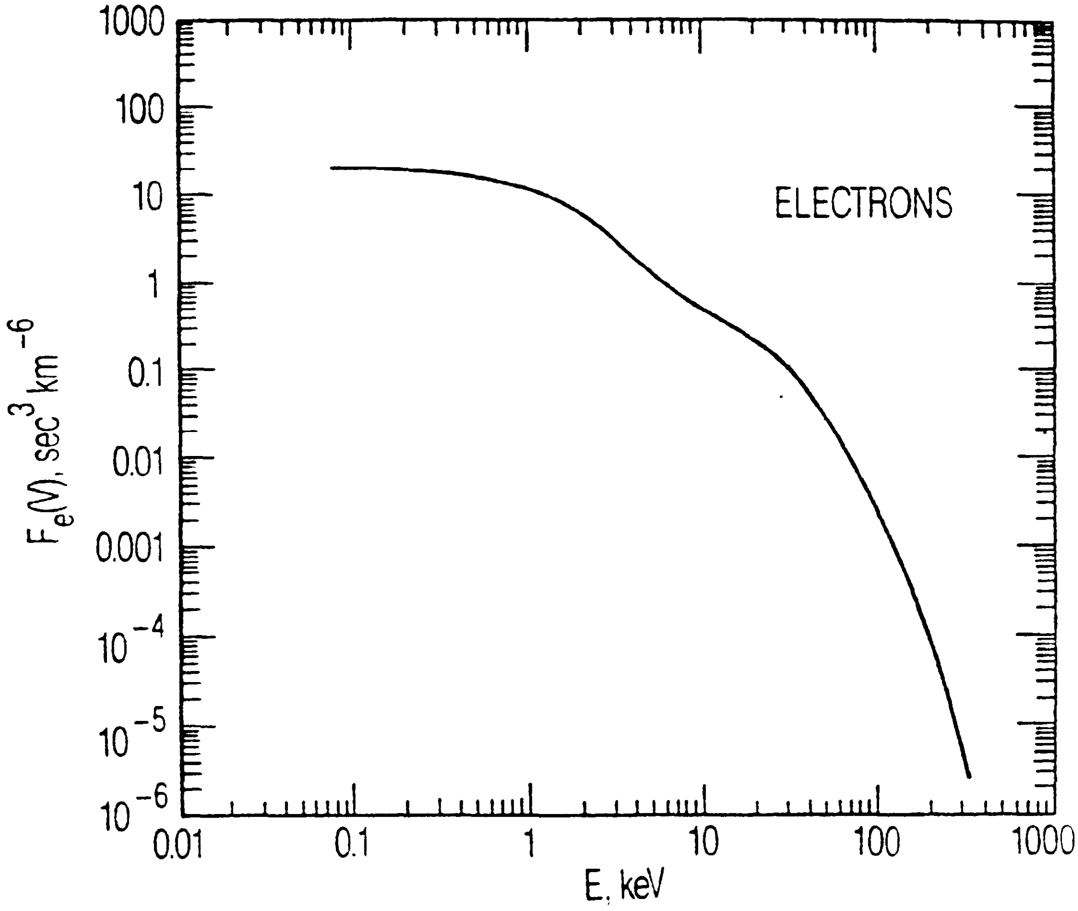


FIGURE 11. Plasma Electron Distribution Function

The corresponding plot of the ion distribution $f_i(v)$ is given in Figure 12. The utilization of these environments for analysis of satellite charging susceptibility and other vehicle-environment interactions are discussed in Chapter 7 of Ref. 6.2 0.

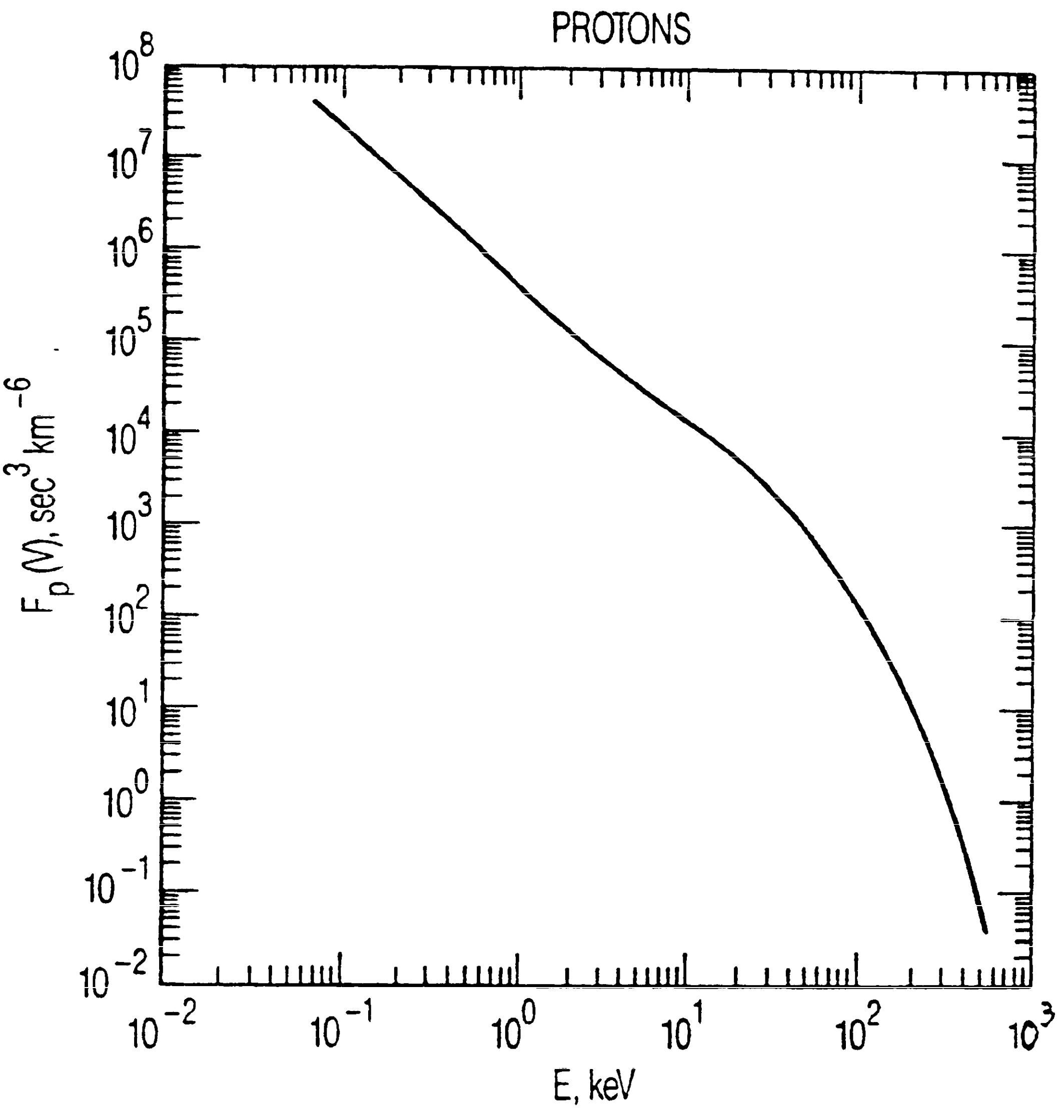


FIGURE 12. Plasma Proton Distribution Function

The satellite orbits above approximately 1000 km and below 25000 km altitude with equatorial- to high-latitude inclinations (O degrees to approximately 60 degrees) are exposed to both an enhanced penetrating radiation (see Paragraph 5.1.2) and enhanced plasma density. There are no statistical models based on data for this plasma regime. There are, however, several theoretical models, all of which are too complicated to include. The plasma density can be crudely, but not accurately, approximated as:

$$N(h,\lambda) = N_i\ [a/(a+h)]^4\ (4 - 3\cos^2 \lambda)^{4/9} \cos^{8/3} \lambda$$

where: h is the satellite altitude in kilometers,

a is the earth's radius in kilometers (6371 km),

$N_i$ is the ionospheric density specified at approximately 770 km altitude at the satellite's longitude and a latitude $\lambda_i$ in the ionosphere given by:

$$\lambda_i = \cos^{-1}(H \cos^2 \lambda),$$

where: $\lambda$ is the satellite latitude, and

$$H = [(a+770\ km)/(a+h)]^{1/2},$$

This approximation ignores the difference between the magnetic latitude and longitude and the geographic latitude and longitude of the satellite. That is, it assumes an Earth-centered magnetic dipole with axis parallel to the Earth's rotation axis. An upper altitude bound, $h_B$, is necessary for the application of the above equation since the plasma density drops sharply at high altitudes. This boundary varies greatly in longitude and time. For the purposes of this standard it is approximated as $h_B = (32,000 \cos^2\lambda)$ km, where $\lambda$ is greater than 60 degrees. Some sample plasma density values, based on a latitude-independent ionospheric density of $2 \times 10^5\ cm^{-3}$, are given in Table V. These values approximate upper limits for the density. Note that the reference ionospheric density Ni is not constant with latitude and must be obtained from an ionospheric model (see Paragraph 5.2.1).

TABLE V. Sample Plasma Density Values

| ORBITAL POSITION Altitude (km) | Latitude (degrees) | DENSITY ($cm^{-3}$) |
|---|---|---|
| 20,000 | 0 | 680 |
| 20,000 | 30 | 600 |
| 20,000 | 50 | 330 |

5.2.3 The Auroral Regions. The aurorae are optical emissions produced by the interaction of precipitating energetic particles with air molecules in the upper atmosphere. The emissions include ultraviolet, visible, and infrared lines, with occasional intensities in excess of several kilo-Rayleighs. The particles originate at very high altitudes and stream along magnetic field lines toward the earth. As the field lines converge at low altitude, the particle intensity is also concentrated. Physical processes may also accel-crate the particles along the field line. The depth in the atmosphere at which the interaction occurs is dependent on the energy of the particle, with 0.1 KeV electrons interacting primarily above 150 km, 1 to 10 KeV electrons in the 80 to 150 km region, and higher energy electrons interacting below 80 km. The occurrence frequency and intensity of aurorae are strongly correlated with magnetic activity. Two general types of aurora occur: discrete and diffuse, with the easily observed discrete aurora being responsible for only about 20 percent of the total particle energy input to the atmosphere in the auroral regions. Discrete aurora extend only 1 to 10 km in latitude at the atmosphere, but may be many km in extent along a contour of magnetic longitude. The majority of discrete aurorae occur in a belt which is local-time dependent, typically covering the latitudinal range of about 60 degrees to 72 degrees (magnetic) at midnight and about 75 degrees to 77 degrees at noon. Diffuse aurora occur in these areas and also to lower latitudes.

For low-altitude polar orbiting satellites, the primary effects of aurorae are three:

a. direct particle impingement on a vehicle as the vehicle passes through an auroral structure;

b. the light emitted by the atmosphere when the particles impinge upon it;

c. modification of the conductivity of the ionosphere in the region of the aurora.

The later is of concern for signal propagation purposes. For space vehicles or space systems that are particularly susceptible to one of these effects, a detailed analysis shall be done. An extensive discussion (Chapter 12 in Ref. 6.2 o) is available as a guide. For relatively insensitive vehicles or systems, the following model of a diffuse aurora shall be used:

Latitudinal intensity distribution: Gaussian with a FWHM of 3.2 degrees

Energy distribution: Gaussian,

$$\phi(E) = \frac{Q}{2(E_m)^3 E^{(-E/E_m)}}$$

where: $\phi(E)$ is in electrons per $cm^2$ sec KeV

E is in KeV

Q is in $ergs/cm^2$-sec

(The minimum, typical, nominal, and maximum values of Q and E shall be as given in Table VI.)

TABLE VI. Diffuse Auroral Energy and Flux Parameters

| | Minimum | Typical | Nominal | Maximum |
|---|---|---|---|---|
| Q | 0.25 | 1.0 | 3.0 | 12.0 |
| Em | 0.40 | 1.5 | 3.0 | 9.0 |

For the purpose of calculating particle impingement (e.g., surface charging), ionospheric modification, and/or light emission effects on satellite performance, the typical values shall be assumed to occur at each auroral zone crossing, the nominal values shall be assumed to occur daily, and the maximum values shall be assumed to occur at monthly intervals. Discrete aurorae shall be modeled as having a Gaussian FWHM -of 0.1 degrees and intensities a factor of ten larger than those in Table VI. If a "severe case" auroral spectrum is required, the following Maxwellian distribution function shall be used (Ref. 6.2 p):

for E equal or less than 17.5 KeV

$$f(E) = 4 \times 10^{-30}\ sec^3 cm^{-6}$$

for E greater than 17.5 KeV

$$f(E) = \frac{N_o (m_e)^{3/2} (E)^{\left(-\frac{E}{k T_o} - \frac{E_o}{}\right)}}{(2\pi k T_o)^{3/2}}$$

where: $N_o = 2\ cm^{-3}$

$kT_o = 4 KeV$

$E_o = 17.5\ KeV$

$m_e$ = rest mass of the electron, $9.11 \times 10^{-28}$ gms, and

f(E) is in units of $sec^3 cm^{-6}$

## 5.3 NEUTRAL ATMOSPHERE.

For the purposes of this Standard, only the region of the neutral atmosphere from 80 km to 1000 km geometric altitude will be considered, effectively defining the thermosphere. The mean state of the thermosphere is taken here as equinoctal for 0900 local time at the equator during a time of average solar EUV (solar 10.7 cm radio emission $F_{10}7$ = 150) and quiet geomagnetic activity (Ap = 4 in MSIS-86, Ref. 6.2 q). Significant perturbations from the mean state occur according to local time, season, latitude, n-year solar cycle and 27-day solar rotation period, and geomagnetic activity. Perturbations are assumed to be negligibly small (factors of two or less) at 80 km and increase with altitude unless otherwise stated. All figures in Subsection 5.3 are MSIS-86 thermosphere model predictions.

5.3.1 Density Above 200 km the density varies approximately sinusoidally during the day with maximum density occurring at 1500 local time. The amplitude of the diurnal variation is a factor of two at 300 km increasing to a factor of five at 600 km; from 80 km to 200 km the density variation is mostly semidiurnal with small amplitude. Seasonal density variations are a factor two or less with a tendency for the greatest values in the summer hemisphere.

The density profile is shown in Figure 13 for solar minimum ( $F_{10.7}$ = 50), mean ($F_{10.7}$ = 150), and maximum ($F_{10.7}$ = 250).

Magnetic storms ($A_p$ = 240) increase density by a factor of four or less with greatest increase poleward of 75 degrees. Storm-induced density variations exhibit great spatial and temporal variability, however. The time constant for exponential return to prestorm values is approximately 12 hours.

5.3.2 Composition. Mean composition profiles for the principal species from 80 km to 600 km are shown in Figure 14; above about 600 km He is the main component. Below about 105 km, the turbopause height, the atmosphere is well mixed at sea-level proportions. Above the turbopause, components are nearly in diffusive equilibrium.

Day-to-night number density ratios are approximately 4, 25, 30, and 80 for O, $O_2$, $N_2$, and Ar above 500 km, and decrease to one at the turbopause. The diurnal variation of lighter constituents is less than a factor of four. Variations are small at all altitudes and latitudes near equinox; they are small at low latitudes throughout the year. At mid and high latitudes, the thermosphere in the winter hemisphere experiences an order of magnitude increase in He from summer values and a factor of two decrease in $O_2$, $N_2$, and Ar from summer values. H and O show only small seasonal variation. Density profiles during solar maximum are shown in Figure 15.

During magnetic storms ($A_p$ = 240), $O_2$, Ar, and $N_2$ increase by a factor of five near the equator and by two orders of magnitude poleward of 75 degrees. Atomic oxygen shows only small variation at all latitudes and H and He decrease by a factor of five. Disturbances begin at high latitudes and spread toward the equator on a time scale of approximately 12 hours, which also characterizes the time scale for exponential return to prestorm conditions.

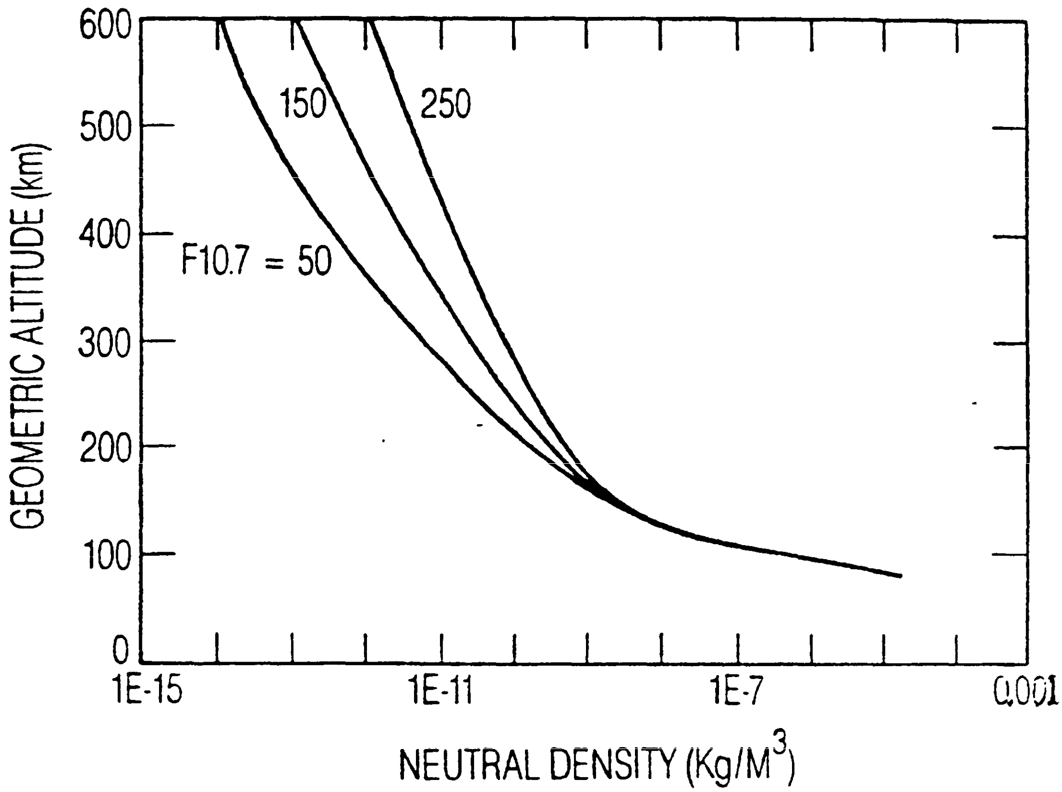


FIGURE 13. Neutral Density at Solar Minimum

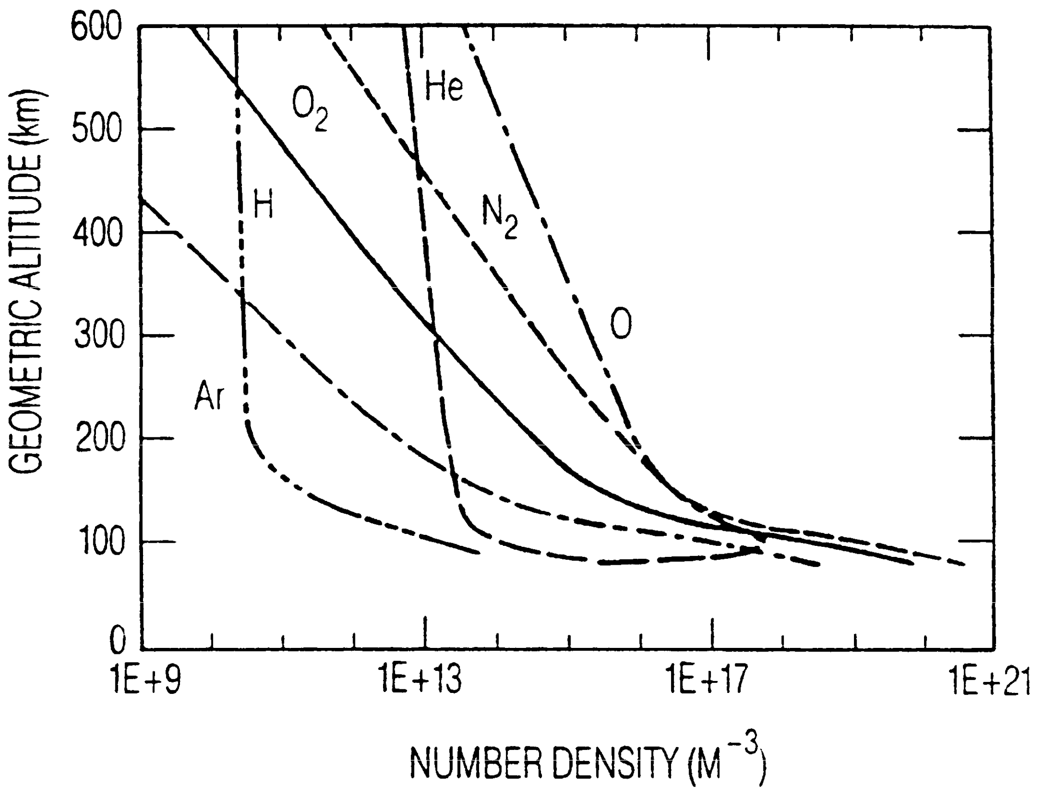


FIGURE 14. Mean Composition Profiles at Solar Minimum

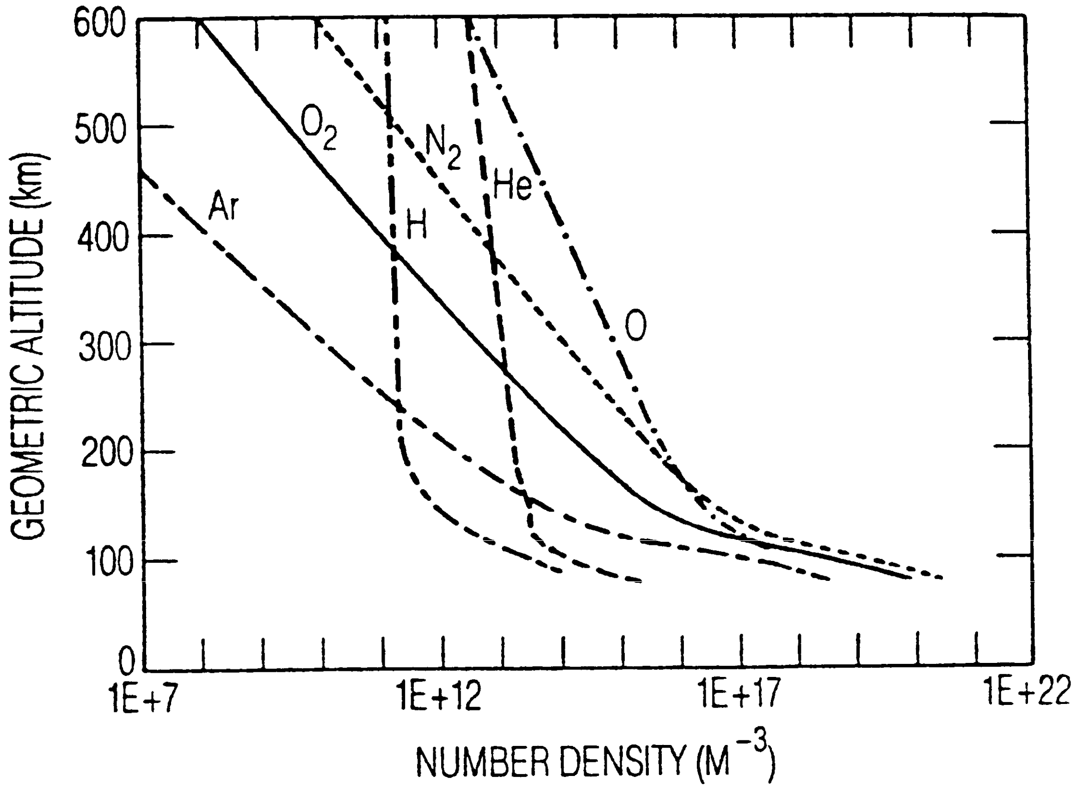


FIGURE 15. Mean Composition Profiles at Solar Maximum

5.3.3 Temperature. Above about 200 km, the temperature varies approximately sinusoidally with local time; the peak temperature occurs at 1500 local time. The diurnal variation of exospheric temperature is approximately ± 15 percent at the equator. The latitude of the diurnal exospheric temperature maximum follows the seasonal variation of solar declination. From 80 km to 200 km the semidiurnal temperature variation dominates with approximately ± 10 percent variation.

The temperature profile variation with solar $F_{10.7}$ is shown in Figure 16 for solar minimum, mean, and maximum. The variation at a particular altitude shall be considered linear with $F_{10.7}$ variation. During active geomagnetic periods the exospheric temperature near the equator increases by 1.5 degrees K times the magnetic index Ap; at high latitudes exospheric temperature increases by 3 degrees K times Ap.

5.3.4 Winds. The neutral thermospheric winds are highly variable, making a mean state difficult to specify. The seasonal latitudinal circulation consists of upwelling over the summer pole and downwelling over the winter pole. Both the summer easterly and winter westerly zonal winds contain a midlatitude jet at about 120 km. Jet core velocities are about 40 m/s and 120 m/s for the easterly and westerly flow, respectively.

Short period wind variations are caused by upward propagating gravity and tidal waves. Gravity waves occur over a wide range of periods and wavelengths and are not subject to prediction, except that gravity wave activity from lower atmosphere forcing is greatest in the winter hemisphere. Local variations of the order of 20 to 40 m/s are characteristic. Tidal winds are also variable. Above about 200 km the diurnal variation dominates with upwelling over the subsolar region and downwelling over the antisolar region; maximum zonal winds in the diurnal circulation are 100 m/s; maximum meridional winds are 100 m/s. Below about 200 km the semidiurnal tide dominates; semidiurnal zonal winds generally increase with altitude from about 10 m/s at 80 km to about 100 m/s above 150 km.

Polar thermospheric winds during magnetic storms, meridional and zonal, may reach 500-1000 m/s; exponential decay time constant is approximately twelve hours.

## 5.4 METEOROIDS.

At any given time, approximately 200 kg of meteoroid material is traveling through the region of space below 2000 km altitude about the Earth. Most of these particles are on the order of 0.1 mm in diameter and are moving at an average relative velocity of 20 km/see.

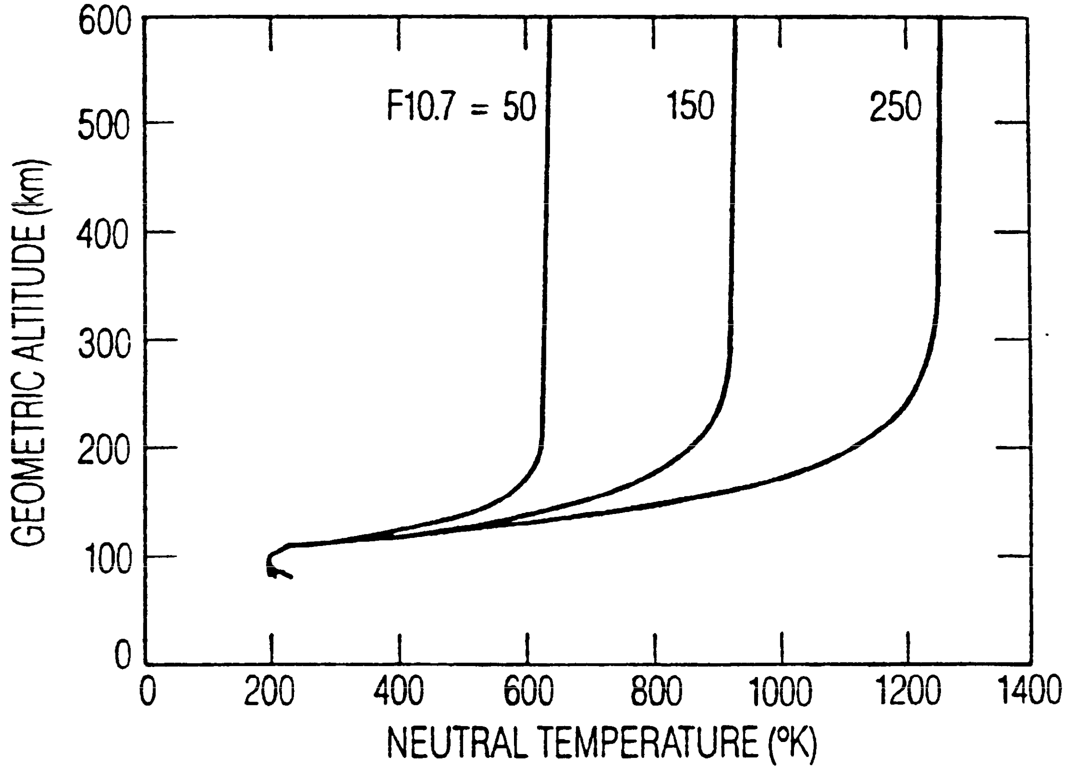


**FIGURE 16.** Neutral Temperature Profile

While man-made debris is not relevant to this Standard, space systems should consider it, since recent measurements indicate that the flux of man-made debris smaller than 1 cm in diameter is comparable to or greater than the meteoroid flux and that while the meteoroid flux is stable, the man-made debris flux is increasing (Refs. 6.2 r and 6.2 s). In low earth orbit, ejects from meteoroid impacts on satellites and effluents from manned space operations constitute the major source of high velocity impacts.

5.4.1 <u>Meteoroid Size, Density, and Distribution</u> Figure 17 presents a curve depicting the meteoroid flux (broken curve). The data presented here are used to determine the number of expected collisions per year between a space vehicle of a given cross-sectional area (perpendicular to the meteoroid's velocity) and meteoroids of a given diameter or larger. The meteoroid flux curve is roughly approximated by the following equation, assuming a meteoroid density of 0.5 gm/cm3:

$$Log_{10}(F) = -14.14 - 1.22\, Log_{10}(m)$$

where F is the cumulative flux (particles/$m^2$-sec)

and m is the mass in grams (valid for $10^{-6}<m<1$).

## 5.5 GEOMAGNETIC FIELD.

The magnetospheric B field is conveniently regarded as a superposition of internal, external, and induction fields. The internal field is regarded as arising from geomagnetic dynamo currents that flow in the Earth's core and (in principle) from crustal concentrations of magnetic material. The external field is regarded as arising from magnetospheric currents and (to a negligible extent) from the partial penetration of the magnetosphere by the solar-interplanetary magnetic field. The induction field results from currents that flow in the ionosphere and in the Earth in response to temporal variations in the magnetospheric currents.

For most space vehicles or space systems, only an internal field component may be required. For orbits with altitudes above about 25000 km, space vehicles may require the addition of an external field component to get more accurate modeling of the actual magnetic field. External field models are available in various configurations. Individual models may consider the tilt of the dipole axis with respect to the solar wind direction, magnetic disturbance conditions, or both. If external field models are to be used, they shall be specified by the user.

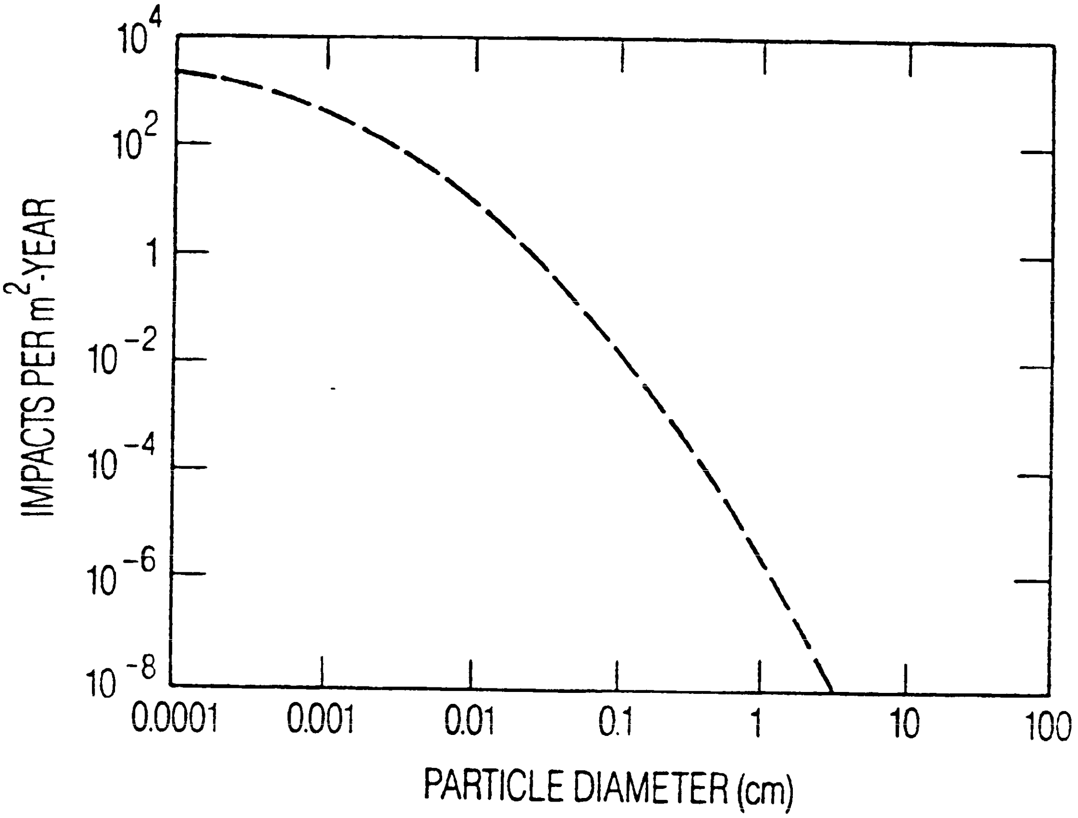


FIGURE 17. Meteoroid Flux Size Distribution

5.5.1 Internal Field The internal magnetic field is represented outside the core as the gradient of a scalar potential expanded in spherical harmonics of degree n and order m (m is equal to or less than n and n is equal to or less than 10). The corresponding Schmidt-normalized expansion coefficients ($g_{mn}$, $h_{mn}$) constitute a model known currently as the IGRF (International Geomagnetic Reference Field, Ref. 6.2 t) and retrospectively as the DGRF (Definitive Geomagnetic Reference Field) for the epoch of interest. Tables of coefficients are published at five-year intervals, the most recent being IGRF85. Time derivatives ($dg_{mn}/dt$, $dh_{mn}/dt$) are included in the IGRF and DGRF for interpolation and extrapolation. Table VII provides the coefficients for IGRF85.

The spherical expansion of the scalar internal field potential is given by:

$$V = (a) \sum_{n=1}^{10} \{a/r\}^{(n+1)} \sum_{m=0}^{n} \{g_n^m \mathrm{Cos}(m\phi) + h_n^m \mathrm{Sin}(m\phi)\} P_n^m \{\mathrm{Cos}\ \theta\}$$

where:

a is the earth radius in km

$P_n^m \{\mathrm{Cos}\ \theta\}$ are the Schmidt functions

$$P_n^m \{\mathrm{Cos}\ \theta\} = \left[\frac{k\ (n-m)!}{(n+m)!}\right]^{1/2} \left[\frac{(1 - \mathrm{Cos}^2\theta)^{m/2}}{2^n!} - \frac{d^{n+m}(\mathrm{Cos}^2\theta - 1)^n}{d(\mathrm{Cos}\ \theta)^{n+m}}\right]$$

where: k = 1 for m = 0

and k = 2 for m greater than 0.

Since B = $-\Delta V$, the Cartesian components X, Y, and Z are:

$$X = \frac{1}{r} \left(\frac{\partial V}{\partial \theta}\right) \quad \text{(northward)}$$

$$Y = \frac{1}{r\mathrm{Sin}\theta} \left(\frac{\partial V}{\partial \phi}\right) \quad \text{(eastward)}$$

$$Z = \left(\frac{\partial V}{\partial r}\right) \quad \text{(downward)}$$

TABLE VII. IGRF85 Internal Field Expansion Coefficients

| n | m | g | h | dg/dt | dh/dt | n | m | g | h | dg/dt | dh/dt |
|---|---|---|---|---|---|---|---|---|---|---|---|
| 1 | 0 | -29988 | | 22.4 | | 8 | 0 | 20 | | 0.8 | |
| 1 | 1 | -1957 | 5606 | 11.3 | -15.9 | 8 | 1 | 7 | 7 | -0.2 | -0.1 |
| | | | | | | 8 | 2 | 1 | -18 | -0.3 | -0.7 |
| 2 | 0 | -1997 | | -18.3 | | 8 | 3 | -11 | 4 | 0.3 | 0.0 |
| 2 | 1 | 3028 | -2129 | 3.2 | -12.7 | 8 | 4 | -7 | -22 | -0.8 | -0.8 |
| 2 | 2 | 1662 | -199 | 7.0 | -25.2 | 8 | 5 | 4 | 9 | -0.2 | 0.2 |
| | | | | | | 8 | 6 | 3 | 16 | 0.7 | 0.2 |
| 3 | 0 | 1279 | | 0.0 | | 8 | 7 | 7 | -13 | -0.3 | -1.1 |
| 3 | 1 | -2181 | -335 | -6.5 | 0.2 | 8 | 8 | -1 | -15 | 1.2 | 0.8 |
| 3 | 2 | 1251 | 271 | -0.7 | 2.7 | | | | | | |
| 3 | 3 | 833 | -252 | 1.0 | -7.9 | 9 | 0 | 6 | | | |
| | | | | | | 9 | 1 | 11 | -21 | | |
| 4 | 0 | 938 | | -1.4 | | 9 | 2 | 2 | 16 | | |
| 4 | 1 | 783 | 212 | -1.4 | 4.6 | 9 | 3 | -12 | 9 | | |
| 4 | 2 | 398 | -257 | -8.2 | 1.6 | 9 | 4 | 9 | -5 | | |
| 4 | 3 | -419 | 53 | -1.8 | 2.9 | 9 | 5 | -3 | -7 | | |
| 4 | 4 | 199 | -298 | -5.0 | 0.4 | 9 | 6 | -1 | 9 | | |
| | | | | | | 9 | 7 | 7 | 10 | | |
| 5 | 0 | -219 | | 1.5 | | 9 | 8 | 1 | -6 | | |
| 5 | 1 | 357 | 46 | 0.4 | 1.8 | 9 | 9 | -5 | 2 | | |
| 5 | 2 | 261 | 149 | -0.8 | -0.4 | | | | | | |
| 5 | 3 | -74 | -150 | -3.3 | 0.0 | 10 | 0 | -3 | | | |
| 5 | 4 | -162 | -78 | 0.2 | 1.3 | 10 | 1 | -4 | 1 | | |
| 5 | 5 | -48 | 92 | 1.4 | 2.1 | 10 | 2 | 2 | 1 | | |
| | | | | | | 10 | 3 | -5 | 2 | | |
| 6 | 0 | 49 | | 0.4 | | 10 | 4 | -2 | 5 | | |
| 6 | 1 | 65 | -15 | 0.0 | -0.5 | 10 | 5 | 5 | -4 | | |
| 6 | 2 | 42 | 93 | 3.4 | -1.4 | 10 | 6 | 3 | -1 | | |
| 6 | 3 | -192 | 71 | 0.8 | 0.0 | 10 | 7 | 1 | -2 | | |
| 6 | 4 | 4 | -43 | 0.8 | -1.6 | 10 | 8 | 2 | 4 | | |
| 6 | 5 | 14 | -2 | 0.3 | 0.5 | 10 | 9 | 3 | -1 | | |
| 6 | 6 | -108 | 17 | -0.1 | 0.0 | 10 | 10 | 0 | -6 | | |
| 7 | 0 | 70 | | -1.0 | | | | | | | |
| 7 | 1 | -59 | -83 | -0.8 | -0.4 | | | | | | |
| 7 | 2 | 2 | -28 | 0.4 | 0.4 | | | | | | |
| 7 | 3 | 20 | -5 | 0.5 | 0.2 | | | | | | |
| 7 | 4 | -13 | 16 | 1.6 | 1.4 | | | | | | |
| 7 | 5 | 1 | 18 | 0.1 | -0.5 | | | | | | |
| 7 | 6 | 11 | -23 | 0.1 | -0.1 | | | | | | |
| 7 | 7 | -2 | -10 | 0.0 | 1.1 | | | | | | |

5.6 ELECTROMAGNETIC

This subsection covers only natural electromagnetic radiation. It does not cover radiation from man-made sources, either spaceborne or radiated from the ground; nor does it cover waves generated by vehicle-plasma interactions.

5.6.1 Magnetospheric Plasma waves The term "plasma wave" is used to identify all waves that are generated in the magnetospheric plasma or whose propagation is strongly affected by the magnetospheric plasma. Plasma waves can be both electromagnetic waves in which energy is exchanged between the electric and magnetic component of the wave or electrostatic waves in which energy is exchanged between the electric field of the wave and charged particles in the plasma. Plasma waves exist in the magnetosphere at all frequencies from ULF to HF. The term also applies to waves generated by lightning. These waves are known as whistlers and propagate extensively within the plasmasphere. Figure 18 (from Tables 20.1 to 20.3 in Ref. 6.2 u) summarizes the expected upper limit for the magnetic and electric energy density in plasma waves within the magnetosphere as a function of frequency.

5.6.2 Terrestrial Radio noise Two principal types of electromagnetic radio emissions come from the terrestrial magnetosphere, auroral kilometric radiation and continuum radiation. Auroral kilometric radiation has an intense peak in the frequency spectrum at about 100 to 300 kHz. This radiation is generated at altitudes of several thousand kilometers in the auroral regions. The upper limit is shown in Figure 19. Continuum radiation is a relatively weak radiation generally in the frequency range from 30 to 110 kHz. It is generated in the outer magnetosphere near the plasmapause. Figure 19, from Ref. 6.2 v, shows the spectrum of both the continuum radiation and the auroral kilometric radiation.

5.6.3 Galactic Radio Noise The sum of all external radio sources in the Milky Way Galaxy produces a relatively uniform source of radio noise known as Galactic Radio Noise. This noise is present in all orbits above the plasma frequency cutoff in the ionosphere. The spectrum of this Galactic Radio Noise is shown in Figure 19.

5.7 SOLAR RADIATIONS.

The solar electromagnetic spectrum shown in Figure 20 shall be used for all space vehicles operating in the magnetospheric environment. These data can be used to calculate the photocurrents from satellite materials. In Figure 20, the continuous component of the spectrum is represented by the

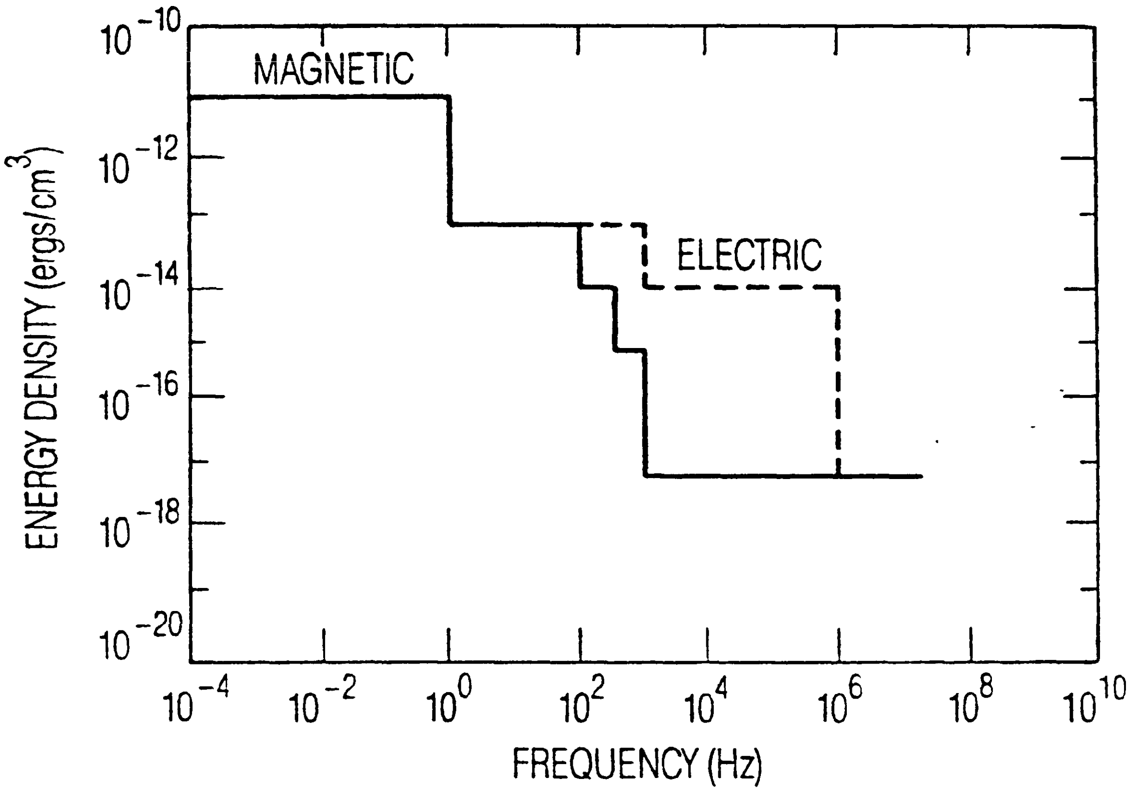


FIGURE 18. Magnetic and Electric Eneray Density

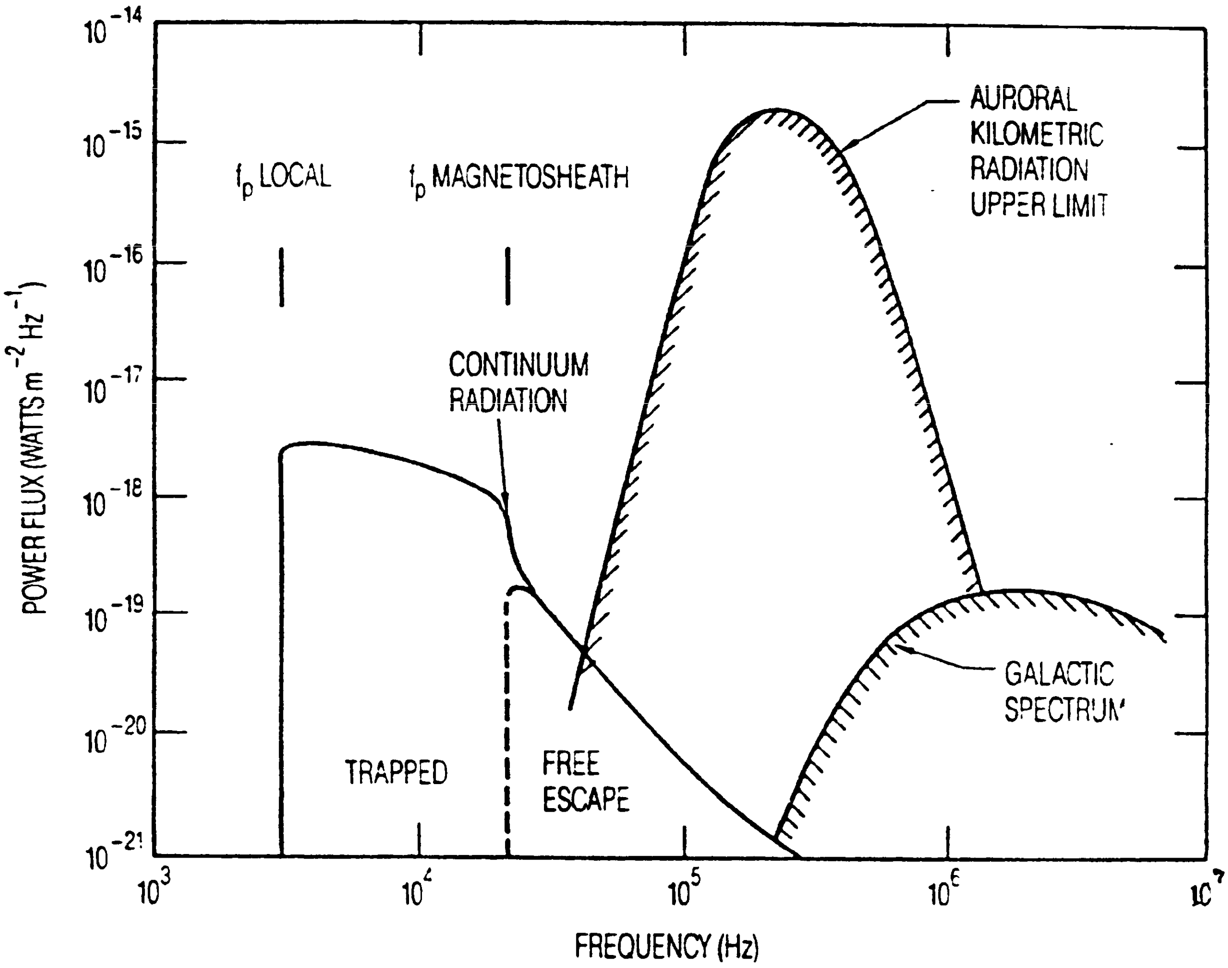


FIGURE 19. Electromagnetic Frequency-power Spectrum

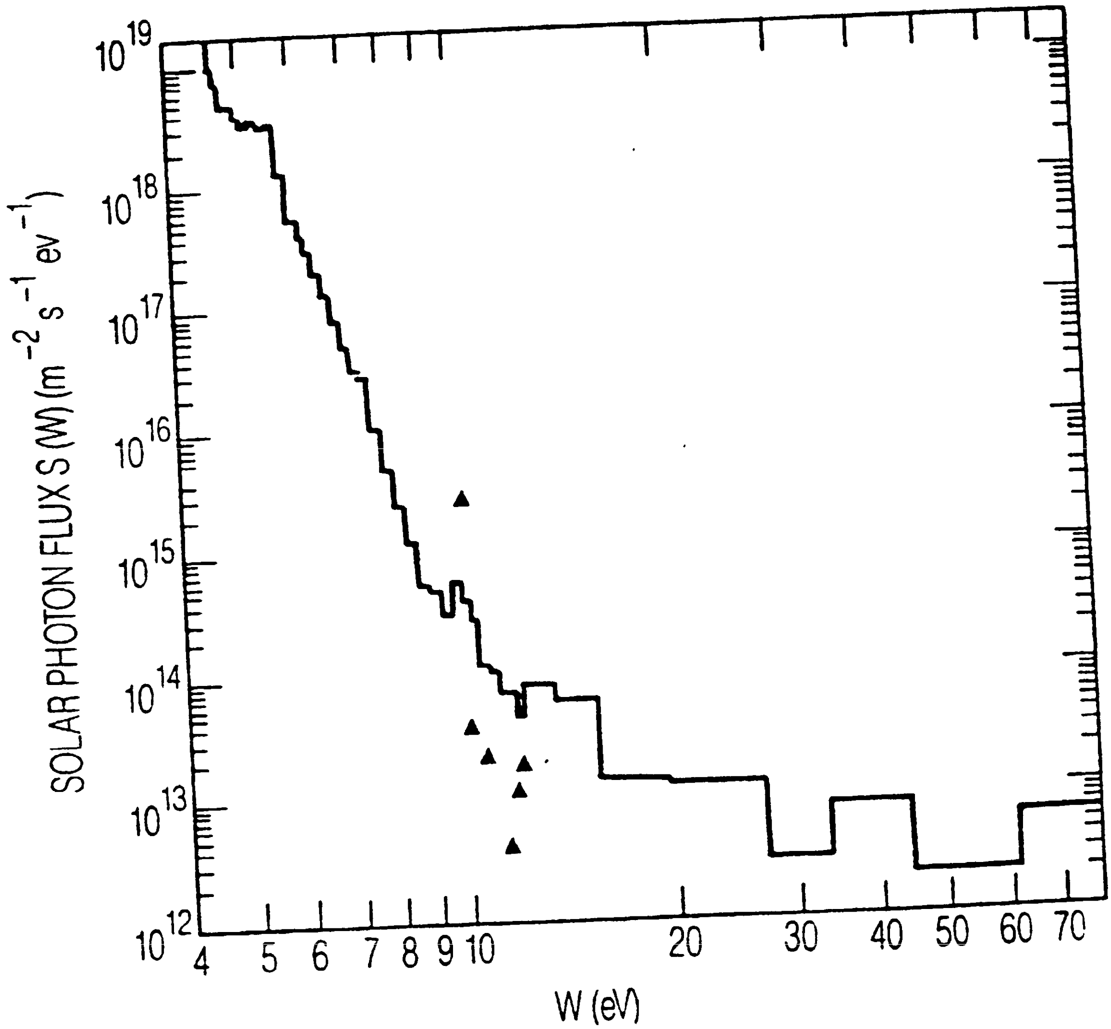


FIGURE 20. Solar Photon Flux Density Spectrum

histogram. The symbols represent the intensity of the important discrete lines in the spectrum which should be added to the continuum by assuming they are formed by a Dirac pulse whose area is represented by the product of the height indicated by the symbol and a width of 1 eV. (e.g., the Lyman-a has a height of $2.7 \times 10^{15}$ photons $sec^{-1}m^{-2}$ (Ref. 6.2 w).

## 5.8 GRAVITATIONAL FIELD.

The accepted gravitational field model for use with Earth-orbiting satellites is defined by the World Geodetic System 1984 (WGS 84), which summarizes physical constants, global geometry, and coefficients of the gravitational potential.

# SECTION 6

# NOTES

The contents of this Notes section are not compliant. The notes are intended for guidance and information only.

## 6.1 INTENDED USE

This standard is intended for use in acquisition contracts for selected space vehicles, upper stage vehicles, payloads, and space experiments. The standard would be cited in the system specifications or other technical requirement documents to specify the natural space environment parameters as applicable to the acquisition.

Note that this standard does not address effects of human operations in space such as orbiting space debris, transmitter radiations, fluid discharges from space vehicles, outgassing, or surface contamination. Neither does it address the interaction between the environment and an orbiting space vehicle, such as atomic oxygen burning of surface materials, surface glow, plasma waves generated by the presence of the space vehicle, space vehicle charging, or orbital dynamics. Nor, finally, does it address the effects of the environment on the space vehicle and subsystems, such as ionizing radiation damage, single event upsets in electronics, or backgrounds such as luminescence and Cerenkov radiation in optical materials. It does, however, provide the necessary environmental parameter data for calculations of space system performance as modified by the presence of these environmental elements.

Although this standard does not address the effects of human operations or the induced environment that is due to the interaction between the environment and a body in space, this should not be interpreted as indicating that these areas are not important. Their effects on a space system may be greater than that due to the natural environment. These areas vary with human activities, tend to be program peculiar, and, therefore, are simply not appropriate for inclusion in this standard. However, these areas should also be included in the analyses of the effects of the total environment on space systems, to the extent they are applicable.

Note that this standard would not normally be used in the acquisition of other types of equipment, such as ground equipment.

## 6.2 GUIDANCE DOCUMENT REFERENCES

a. Tsao, C. H. et al,"Cosmic Ray Effects on Microelectronics, Part I: The Near-Earth Particle Environment", NRL Memorandum Report 4506, 1981 (NTIS Accession No. AD-A103897). (5.1.1.1)

b. Adams, J. H., Jr., J. R. Letaw, and D. F. Smart, "Cosmic Ray Effects on Microelectronics, Part II: The Geomagnetic Cutoff Effects", NRL Memorandum Report 5099, 1983 (NTIS Accession No. AD-A128601). (5.1.1.1)

c. Adams, J. H., Jr., et al, "Cosmic Ray Effects on Microelectronics, Part III: Propogation of Cosmic Rays in the Atmosphere", NRL Memorandum Report 5402, 1984. (5.1.1.1)

d. Adams, J. H., Jr., "Cosmic Ray Effects on Microelectronics, Part IV", NRL Memorandum Report 5901, 1986. (5.1.1.1)

e. McIlwain, Carl E., "Coordinates for Mapping the Distribution of Magnetically Trapped Particles," J. Geophys. Res., 66, 3681-3691, 1961. (5.1.2)

f. Sawyer, D. M., and J. I. Vette, "AP-8 Trapped Proton Environment", NSSDC WDC-A-R&S 76-06, 1976. (5.1.2.1.1, 5.1.2.2.1, 5.1.2.3.1, 5.1.2.4.1, 5.1.2.5.1)

g. Konradi, A. and A. C. Hardy, "Radiation Environment Models and the Atmospheric Cutoff" J. Spacecraft and Rockets, 24, p. 284, 1987. (5.1.2.1.1.1)

h. Teague, M. J., K. W. Chan and J. I. Vette, "AE-6: A Model Environment of Trapped Electrons for Solar Maximum", NSSDC WDC-A-R&S 76-04, 1976. (5.1.2.1.2, 5.1.2.2.2)

i. Vette, J. I. and A. B. Lucero, "Models of the Trapped Radiation Environment, Vol. III: Electrons at Synchronous Altitudes", NASA SP-3024, 1967. (5.1.2.3.2, 5.1.2.5.2)

j. Vette, J. I., K. W. Chan and M. J. Teague, "Problems in Modeling the Earth's Trapped Radiation Environment", AFGL-TR-78-0130, 1978 (NTIS Accession No. AD-A059273). (5.1.2.4.2)

k. Rawer, K., "International Reference Ionosphere -IRI-79", Ed. J. V. Lincoln and R. O. Conkright, WDC-A-STP, NOAA, Boulder, CO, 1981. (5.2.1.1)

l. Rawer, K., "International Reference Ionosphere", Adv. Space Res., 2, No. 10, 181-257, 1982. (5.2.1.1)

m. Dana, R. A., and D. L. Knapp, "The Impact of Strong Scintillation on Space Based Radar Design II: Noncoherent Detection", IEEE Trans. Aerospace and Electronic Systems, AES-22, 34-46, 1986. (5.2.1.2)

n. Fremouw, E. J., and R. E. Robins, "An Equatorial Scintill-ation Model", DNS TR-85-333, September 1985. (5.2.1.2)

o. Handbook of Geophysics and the Space Environment, Air Force Geophysics Laboratory, A. S. Jursa ed., 1985. NTIS ADA 167000. (5.2.2.1, 5.2.3)

p. Yeh, H., -C. and M. S. Gussenhoven, "The Statistical Electron Environment for Defense Meteorological Satellite Program Eclipse Charging," J. Geophys Res., 92, 7705-7715, 1987. (5.2.3)

q. Hedin, A. E., "MSIS-86 Thermospheric Model", J. Geophys. Res. 92, 4649-4662, 1987. (5.3)

r. USAF Advisory Board, "Current and Potential Technology to Protect Air Force Space Missions from Current and Future Debris," December 1987. (5.4)

s. Howell Jr., L. W., "A Stochastic Model for Particle Impingements on Orbiting Spacecraft," J. Astro. Sci., 34, No. 4, Oct-Dec 1986, pp. 375-401. (5.4)

t. IAGA Division 1, Working Group 1, International Geomagnetic Reference Field revision 1985, Eos, Trans. Am. Geophys. Union, 67, 523-524, 1986. (5.5.1)

u. S. D. Shawhan, "Magnetospheric Plasma Wave Research 1975-1978", in Reviews of Geophysics and Space Physics, 17, 705, 1979. (5.6.1)

v. D. A. Gurnett, "The Earth as a Radio Source, in Magnetospheric Particles and Fields", edited; B. M. McCormac; D. Reidel Publishing Co., Dordrecht-Holland, p.197-208, 1976. (5.6.2)

w. Grard, R. J. L., "Properties of the Satellite Photoelectron Sheath Derived from Photoemission Laboratory Measurements", J. Geophys. Res., 68, 78, p. 2885, 1973. (5.7)

x. ANSI/AIAA G-003-1990, "Guide to Reference and Standard Atmosphere Models", American Institute of Aeronautics and Astronautics, 1990.

## 6.3 TAILORED APPLICATION

The technical requirements in each contract should be tailored to the needs of that particular acquisition. Military specifications and standards need not be applied in their entirety. Only the minimum requirements needed to provide the basis for achieving the program requirements should be imposed. The cost of imposing each requirement of this standard should be evaluated by the program office against the benefits that should be realized. However, the risks and potential costs of not imposing requirements must also be considered.

Contractors are encouraged to report to the contracting officer, for program office review and consideration, those specific requirements that seem inappropriate, are believed excessive, or are conflicting with other contract requirements. However, contractors are reminded that any departure from contractually imposed requirements can be granted only by the contracting officer.

## 6.4 SUBJECT TERM (KEY WORD) LISTING

Atmosphere
Cosmic Rays
Electrons
Environment
Geomagnetic Field
Gravitational Field
Ionosphere
Meteoroids
Particles
Protons
Radiation Belts
Radio Noise
Scintillation
Solar Storm
Space
Thermosphere

Custodians
Air Force - 19

Preparing Activity
Air Force - 19

(Project No. 1810-F045)
Document 1977b/Arch 1495b

# INDEX

PAGE

INDEX
(continued)

# STANDARDIZATION DOCUMENT IMPROVEMENT PROPOSAL

**INSTRUCTIONS**

1. The preparing activity must complete blocks 1, 2, 3, and 8. In block 1, both the document number and revision letter should be given.
2. The submitter of this form must complete blocks 4, 5, 6, and 7.
3. The preparing activity must provide a reply within 30 days from receipt of the form.

NOTE: This form may not be used to request copies of documents, nor to request waivers, or clarification of requirements on current contracts. Comments submitted on this form do not constitute or imply authorization to waive any portion of the referenced document(s) or to amend contractual requirements.

| I RECOMMEND A CHANGE: | 1. DOCUMENT NUMBER<br>MIL-STD-1809 (USAF) | 2. DOCUMENT DATE (YYMMDD)<br>91 02 15 |
|---|---|---|

3. DOCUMENT TITLE
Space Environment for USAF Space Vehicles

4. NATURE OF CHANGE *(Identify paragraph number and include proposed rewrite, if possible. Attach extra sheets as needed.)*

5. REASON FOR RECOMMENDATION

6. SUBMITTER

| a. NAME *(Last, First, Middle Initial)* | b. ORGANIZATION | |
|---|---|---|
| c. ADDRESS *(Include Zip Code)* | d. TELEPHONE *(Include Area Code)*<br>(1) Commercial<br>(2) AUTOVON<br>*(If applicable)* | 7. DATE SUBMITTED *(YYMMDD)* |

8. PREPARING ACTIVITY

| a. NAME<br>USAF Space Systems Division<br>SSD/SDMS | b. TELEPHONE *(Include Area Code)*<br>(1) Commercial (213) 363-3234<br>(2) AUTOVON |
|---|---|
| c. ADDRESS *(Include Zip Code)*<br>P.O. Box 92960<br>Los Angeles, CA 90009-2960 | IF YOU DO NOT RECEIVE A REPLY WITHIN 45 DAYS, CONTACT:<br>Defense Quality and Standardization Office<br>5203 Leesburg Pike, Suite 1403, Falls Church, VA 22041-3466<br>Telephone (703) 756-2340 AUTOVON 289-2340 |